Biogeosciences Discuss., 11, 10779–10826, 2014
www.biogeosciences-discuss.net/11/10779/2014/
doi:10.5194/bgd-11-10779-2014

Biogeosciences Discussions
Open Access

HESFIRE: an explicit fire model for projections in the coupled Human–Earth System

Y. Le Page[1], D. Morton[2], B. Bond-Lamberty[1], J. M. C. Pereira[3], and G. Hurtt[4]

[1]Pacific Northwest National Laboratory, Joint Global Change Research Institute, University of Maryland, College Park, MD 20740, USA
[2]NASA Goddard Space Flight Center, Greenbelt, MD 20771, USA
[3]Centro de Estudos Florestais, Instituto Superior de Agronomia, Universiadade de Lisboa, Tapada da Ajuda, 1349-017 Lisbon, Portugal
[4]Department of Geographical Sciences, University of Maryland, College Park, MD 20740, USA

Received: 23 May 2014 – Accepted: 2 June 2014 – Published: 14 July 2014

Correspondence to: Y. Le Page (yannick.lepage@pnnl.gov)

Published by Copernicus Publications on behalf of the European Geosciences Union.

Abstract

Vegetation fires are a major driver of ecosystem dynamics and greenhouse gas emissions. Potential changes in fire activity under future climate and land use scenarios thus have important consequences for human and natural systems. Anticipating these consequences relies first on a realistic model of fire activity (e.g. fire incidence and inter-annual variability) and second on a model accounting for fire impacts (e.g. mortality and emissions). Key opportunities remain to develop the capabilities of fire activity models, which include quantifying the influence of poorly understood fire drivers, modeling the occurrence of large, multi-day fires – which have major impacts – and evaluating the fire driving assumptions and parameterization with observation data. Here, we describe a fire model, HESFIRE, which integrates the influence of weather, vegetation characteristics, and human activities in a standalone framework, with a particular emphasis on keeping model assumptions consistent with fire ecology, such as allowing fires to spread over consecutive days. A subset of the model parameters was calibrated through an optimization procedure using observational data to enhance our understanding of regional drivers of fire activity and improve the performance of the model on a global scale. Modeled fire activity showed reasonable agreement with observations of burned area, fire seasonality and inter-annual variability in many regions, including for spatial and temporal domains not included in the optimization procedure. Significant discrepancies – most notably regarding fires in boreal regions, in xeric ecosystems, and fire size distribution – are investigated to propose model development strategies. We highlight the capabilities of HESFIRE and its optimization procedure to analyze the sensitivity of fire activity, and to provide fire projections in the coupled Human–Earth System at regional and global scale. These capabilities and their detailed evaluation also provide a solid foundation for integration within a vegetation model to represent fire impacts on vegetation dynamics and emissions.

BGD
11, 10779–10826, 2014

BGD
11, 10779–10826, 2014
HESFIRE
Y. Le Page et al.

1 Introduction

The human population has more than doubled in the past 50 years, expanding the scale and diversity of changes in the Earth system from anthropogenic activity. The build-up of greenhouse gases in the atmosphere, as well as the degradation and conversion of natural lands, have major consequences for future climate, natural ecosystems, and human societies (Parry, 2007; Stocker et al., 2013). The interactions between human and natural systems are complex, yet observational data, field experiments, and various types of models continue to elucidate key linkages among climate variability, ecosystem function, and anthropogenic activities. This knowledge is essential to anticipate potential changes under future conditions and to design adaptation or mitigation strategies that promote the sustainability of the coupled Human–Earth System.

One of these interactive processes linking human activities and natural ecosystems is fire (Bowman et al., 2009). Humans exert considerable influence over global fire activity (Le Page et al., 2010a); fire-driven deforestation accounts for an estimated 20 % of the increase in atmospheric CO_2 from human activities since preindustrial times (Bowman et al., 2011; van der Werf et al., 2010). Fire activity depends on a range of drivers covering three major components of the Human–Earth System: the atmosphere (e.g. weather conditions), the terrestrial biosphere (e.g. fuel loads) and anthropogenic activities (e.g. land-use fires and fire suppression). The interaction among these drivers determines global fire activity, as illustrated in 1997–1998 when a strong El Niño led to extreme fire events around the world (Le Page et al., 2008), including unprecedented fires in peatlands and forests of Indonesia where human-caused fires emitted an estimated 13 to 40 % of the world's annual fossil fuel emissions (Page et al., 2002).

Future fire activity and impacts thus depends on the synergistic interactions these drivers, and on fire-mediated feedbacks in the Earth system. In boreal regions, recent increases in fire activity are consistent with warming and drying trends that favor fire occurrence (Gillett et al., 2004, 2005). Projected increases in fire activity from climate change in other ecosystems range from a moderate decrease to a 5-fold increase depending on characteristics of the climate projections and modeling frameworks (e.g. Flannigan et al., 2009; Liu et al., 2010; Soares-Filho et al., 2012). Studies that consider both climatic and anthropogenic drivers highlight the sensitivity of future fire activity to societal developments, including fire suppression and fire-driven deforestation of natural ecosystems for agricultural expansion (Cardoso et al., 2003; Keeley and Fotheringham, 2003; Kloster et al., 2012; Le Page et al., 2010b). In return, altered fire activity may amplify or moderate climate change via global greenhouse gas emissions and local albedo changes (Liu et al., 2013; Randerson et al., 2006). Net changes in carbon emissions from disturbance, including fires, constitute a major uncertainty for climate change adaptation and mitigation assessments: any unforeseen increase in greenhouse gas emissions from fire would require an adaptive mitigation effort to achieve a predefined climate target (Le Page et al., 2013; Running, 2008).

Modeling changes in fire activity under future climate, policy, and land use scenarios requires a framework with a broad range of variables (Pechony and Shindell, 2009) and a good understanding of the influence of these variables for model parameterization. A range of global fire models have been developed, each with a different focus (e.g. Arora and Boer, 2005; Li et al., 2013a; Pfeiffer et al., 2013; Prentice et al., 2011; Thonicke et al., 2001, 2010). Among these examples, SPITFIRE (Thonicke et al., 2010) is a process-based fire model coupled to a vegetation model explicitly representing many physical properties of fire behavior providing great capabilities regarding fire spread, fire intensity and fire impacts (damage, mortality, emissions). The model developed by (Li et al., 2013a) has a particular emphasis on depicting anthropogenic ignitions, with good performances regarding global patterns of burned area.

One key prospect to build upon existing work, as mentioned by Thonicke et al. (2010), is to develop the capability for modeling fire spread over consecutive days. This capability has been reported in one global fire model focusing on pre-industrial era fires (Pfeiffer et al., 2013). In many ecosystems, multi-day fires are a major driver of the overall fire activity. Dry-spells and heat-waves in days and weeks following ignition enable the growth of large fires in boreal regions (Abatzoglou and Kolden, 2011), and although those burning over 200 ha represent only ~3 % of all fires, they account for ~97 % of the total area burned (Stocks et al., 2002). Large-scale climate anomalies in tropical forests allow individual fires to burn large areas of intact tropical forests over the course of several weeks, including areas further away from the forest edge where ignition typically occurs (Morton et al., 2013). Similar findings have been reported for temperate regions, including in Mediterranean ecosystem (Pereira et al., 2005; Westerling et al., 2004). Modeling fire-climate interactions therefore requires careful attention to the duration of fire weather events.

Another opportunity for fire modeling research is model parameterization and their evaluation. Many early models had to extrapolate findings from local studies or to simplify key drivers of fire activity when information of some components was unavailable (e.g. ignitions independent of anthropogenic activities). Recently, model calibration has been applied to one (Thonicke et al., 2010) or a few (Li et al., 2013a) parameters. Expanding this approach to additional parameters in a model with realistic assumptions on key aspects of fire ecology could yield relevant insights on fire drivers. Subsequent model evaluation is essential to assess our confidence in fire projections, especially regarding fire activity – which global spatio-temporal patterns are relatively well characterized by observation data (Mouillot et al., 2014) – because depicting patterns of fire activity and their sensitivity to fire drivers is a pre-requisite to project realistic fire impacts. Evaluating fire models is challenging when they are embedded within vegetation models however, because vegetation distribution strongly affects fire dynamics (Scott and Burgan, 2005), and if inaccurate (e.g. Fig. 7 in Sitch et al., 2003, Fig. 2 in Cramer et al., 2001), may lead to unrealistic fire projections for reasons unrelated to the fire parameterization.

This paper describes the development of a fire model, HESFIRE (Human–Earth System FIRE), to improve our understanding of current fire activity and our capacity to anticipate its evolution with future changes in the coupled Human–Earth system. HESFIRE is first developed as a standalone model, i.e. not integrated within a dynamic vegetation model. The major emphasis of this research is to outline the fundamental

BGD
11, 10779–10826, 2014

structure of the model and apply an optimization procedure to explore some of the research opportunities mentioned above. Our analysis has three main objectives: (1) explicit representation of fire ignition, spread, and termination, with realistic assumptions regarding fire ecology (e.g. multi-day fires); (2) consideration of atmospheric, terrestrial, and anthropogenic drivers in order to represent synergistic effects among changes in climate, vegetation, and human activity – key steps towards the implementation of the fire model within coupled Human–Earth system models; and (3) model optimization and evaluation to improve our understanding of constraints on global fire activity and to quantify uncertainties of future fire activity projections.

2 Methods

2.1 Model overview

The model structure was designed to satisfy objectives 1 and 2 (realistic assumptions and ease of integration to vegetation and integrated assessment models), and some of its parameters were mathematically optimized to estimate the quantitative role of poorly understood drivers and to maximize the agreement between modeled and observed fire regimes (objective 3). It focuses on fires in natural ecosystems: deforestation and agricultural fires are dependent on very different dynamics (controlled spread, pile burning) and thus only considered as a source of ignition for escaped fires.

The model is organized in three parts, with specific drivers for fire ignition, spread, and termination (Fig. 1):

- Fire ignitions. Natural ignitions are a function of cloud-to-ground lightning strikes and a probability of ignition per strike. Human ignitions reflect agricultural and ecosystem management as a function of land use density and national Gross Domestic Product (GDP).

BGD
11, 10779–10826, 2014

- Fire spread. Fire spread rate is a function of weather conditions (relative humidity, temperature, wind speed), soil moisture, and fuel structure categories (forest, shrub, grass).
- Fire termination. Four factors control the termination of fires: weather conditions, fuel availability, landscape fragmentation, and fire suppression efforts (a function of land use, GDP and fire intensity).

To account for the diurnal variability in fire spread and termination (see introduction), every fire is tracked individually with a 12 h timestep. The analyses presented in this paper were conducted with model runs at a resolution of 1°.

HESFIRE was coded in Python 2.7 and is freely available at https://github.com/HESFIRE/model (note: code currently being finalized for shared access, will be uploaded before potential publication). The optimization procedure is included in the code.

2.2 Model description

The full list of parameters is described in Table 1. The following sections detail the fire ignition, spread and termination modules.

2.2.1 Fire ignitions

Fires may occur due to both natural and human ignitions:

$$N_{\text{fires}} = \text{NATign} + \text{LUign} \tag{1}$$

To introduce some of the stochasticity associated with fires, N_{fires} represents the expected realization of a Bernoulli trial ($n = 1000$), and the final number of ignitions is computed following the actual trial.

BGD
11, 10779–10826, 2014

Natural ignitions

Lightning strikes are the most frequent source of natural ignitions. Lightning ignitions are highly stochastic because of the localized characteristics of convective storms, variability in the frequency of cloud-to-ground lightning, and coincident rainfall which can terminate fires ignited by lightning before substantial spread occurs (see review in Podur et al., 2003). In HESFIRE, natural ignitions are the product of cloud-to-ground lightning strikes, the probability of ignition from lightning, and the fractional cover of flammable vegetation in a given grid cell:

$$\mathrm{NATign} = \mathrm{CG_{flashes}} \cdot \mathrm{CG_{firep}} \cdot (1 - \mathrm{Frag_n}) \quad (2)$$

Where $CG_{flashes}$ is the number of cloud-to-ground lightning strikes, CG_{firep} is the ignition probability determined through the optimization procedure (see Sect. 2.3), and $Frag_n$ (fragmentation) the fraction of the grid-cell that cannot sustain a fire (non-natural land or not enough fuel, see later).

Anthropogenic ignitions

Humans are the dominant source of fire ignition in most temperate and tropical ecosystems. Ignitions from human activities include fires for agriculture and ecosystem management, deforestation for agricultural expansion, accidental fires, and arson. Fire usage varies across countries, climate zones, and land use practices (Korontzi et al., 2006; Le Page et al., 2010a), and this diversity of human activity cannot be fully captured with current knowledge and data. However, wealth is an important driver of fire use in agricultural settings, since fire is typically the least costly tool to clear natural vegetation, control pests, or increase soil fertility (Laris, 2002; Thrupp et al., 1997). Thus we represent anthropogenic ignitions as a function of land use intensity and national GDP, where higher fractional land use and lower GDP increase anthropogenic fire ignitions. Similar to the approach used in the SPITFIRE model (Thonicke et al., 2010),

BGD
11, 10779–10826, 2014
HESFIRE
Y. Le Page et al.

we assume that initial settlements bring more ignitions relative to additional ones:

$$\text{Humign} = (1 - \text{GDP}_n)^{\text{GDPexp}} \cdot \int_0^{\text{LU}} \text{LUign} \cdot \text{LU} \cdot (1 - \text{LU}_n)^{\text{LUexp}} \quad (3)$$

where GDP_n is the normalized Gross Domestic Product per capita (from 0$ to 60 000$), GDP_{exp} the associated shape parameter, LUign is the number of ignitions per km^2 of land use, LU the land use area in the grid-cell considered, and LU_{exp} the shape parameter controlling the decrease in the amount of additional ignitions with incremental land use. LU_n is the normalized land use fraction of the grid-cell, from 0 to 0.1 only, as applying a normalization to higher fractions systematically led to very high values of the optimized parameter LU_{exp}, pointing to a rapid saturation of human ignitions with land use density. We thus progressively applied a narrower normalization interval to get a better depiction of the relationship. LUign and GDP_{exp} were also determined through our optimization procedure. Eq. (3) conveys the following fire driving mechanisms:

- Human ignitions increase with human occupation of the landscape, but saturate once 10 % of the landscape is occupied.

- Fire use for land use management depends on the regional GDP, with maximum fire use in the poorest regions, and virtually no fire use at all for regions beyond 60 000$/capita. We thus assume that the few countries with a current GDP beyond 60 000$/capita have no human ignitions. In the future, we plan to consider land use and arson or unintentional fire ignitions separately, the latter being parameterized independently from GDP.

2.2.2 Fire spread

The rate of fire spread is modeled for three broad vegetation types – forest, shrub, and grass – and varies as a function of relative humidity, soil moisture, temperature, wind speed, and fuel structure. Maximum fire spread rates are constrained by observations

BGD
11, 10779–10826, 2014
HESFIRE
Y. Le Page et al.

(Scott and Burgan, 2005): 0.28 m s^{-1} in forests, 1.12 m s^{-1} in shrubs, and 2.79 m s^{-1} in grasses. The actual rate of fire spread F_{rate} for each vegetation type is then computed:

$$F_{\text{rate}} = \text{Max}_{\text{rate}} \cdot \left(1 - \text{RH}_{\text{n}}^{\text{RH}_{\text{exp}}}\right) \cdot \left(1 - \text{SW}_{\text{n}}^{\text{SW}_{\text{exp}}}\right) \cdot \left(1 - T_{\text{n}}^{T_{\text{exp}}}\right) \cdot G(W) \tag{4}$$

Where RH_n, SW_n and T_n are normalized relative humidity (from 30–80 %), soil moisture (20–35 %) and temperature (0–30 °C) over a 12 h period, and $G(W)$ is a function of wind speed (see below). RH_{exp}, SW_{exp} and T_{exp} are the optimized shape parameters controlling the fire-driving relationship. The influence of wind on fire spread rate, $G(W)$, is computed following the method described in (Li et al., 2012), as a function of the length-to-breadth (LB) and head-to-back (HB) ratios of a typical elliptical burned area, both of which depend on wind speed (w).

$$\text{LB} = 1 + 10 \cdot (1 - e^{-0.06 \cdot \omega}) \tag{5}$$

$$\text{HB} = \text{LB} + \frac{\text{LB} + (\text{LB}^2 - 1)^{0.5}}{\text{LB} - (\text{LB}^2 - 1)^{0.5}} \tag{6}$$

$$G(W) = 2 \cdot \frac{\text{LB}}{(1 + 1/\,\text{HB})} \cdot 0.0455 \tag{7}$$

Within a grid cell, fires are assumed to spread with equal probability to each of the three vegetation types. Their respective burned area therefore reflects their specific fire spread rates and fraction within the grid-cell. Given the large size of model grid cells (1° × 1°), fire spread to neighboring grid-cells is not considered.

2.2.3 Termination

Individual, multi-day fires are modeled from ignition to termination. Fire termination may occur in 4 ways: weather conditions are no longer favorable to fire spread, the fire is stopped by landscape fragmentation, by lack of fuel, or suppressed by fire-fighting activities. Each termination pathway contributes to the overall probability of termination; fire termination is then determined by the same Bernoulli trial stochastic approach applied to fire ignitions. Fire termination is computed every 12 h and may occur before any spread (i.e., right after ignition).

$$\mathrm{Nfires}_{t+1} = \mathrm{Nfires}_t \cdot \left\{ \begin{array}{l} (1 - \mathrm{Fuel}_{\mathrm{termp}}) \cdot (1 - \mathrm{Frag}_{\mathrm{termp}}) \cdot \\ (1 - \mathrm{Supp}_{\mathrm{termp}}) \cdot (1 - \mathrm{Weather}_{\mathrm{termp}}) \end{array} \right\} \tag{8}$$

where Nfires is the number of active fires, $\mathrm{Fuel}_{\mathrm{termp}}$, $\mathrm{Frag}_{\mathrm{termp}}$, $\mathrm{Supp}_{\mathrm{termp}}$ and $\mathrm{Weather}_{\mathrm{termp}}$, are the probability of termination due to each factor.

Weather-related termination occurs when fire spread rate decreases to zero, that is when RH is 80 % or above, soil moisture is 35 % or above, or when the temperature drops below freezing.

Fuel load and its impact on termination is a function of the cumulative precipitation prior to the current time step, as an indicator of water limitation on fuel build-up in arid areas:

$$\mathrm{Fuel}_{\mathrm{termp}} = 1 - \mathrm{Precip}_{\mathrm{n}}^{\mathrm{FUELexp}} \tag{9}$$

where $\mathrm{Precip}_{\mathrm{n}}$ is the average precipitation from −15 to −3 months, normalized from 0.5 mm day^{-1} ($\mathrm{Precip}_{\mathrm{n}} = 1$) to 3 mm day^{-1} ($\mathrm{Precip}_{\mathrm{n}} = 0$). These were chosen as the best of several trial configurations with different precipitation accumulation periods and normalization ranges. $\mathrm{Fuel}_{\mathrm{exp}}$ is the shape parameter, determined through the optimization procedure. Note that when integrated into an ecosystem model, fuel constraints can be directly inferred from vegetation, litter and soil carbon pools.

Landscape fragmentation is computed as the fraction of the grid-cell that cannot sustain natural vegetation fires (croplands, urban areas, water bodies, deserts). Burned areas also contribute to fragmentation, up to 8 months after the fire, thus avoiding repeated burns within the same fire season, but allowing fuel build-up for the following fire season if enough precipitation occurs (e.g. in sub-Saharan Africa).

$$\mathrm{Frag}_{\mathrm{termp}} = \mathrm{Frag}_{\mathrm{n}}^{\mathrm{FRAGexp}} \tag{10}$$

BGD
11, 10779–10826, 2014
HESFIRE
Y. Le Page et al.

where Frag_n is the fraction of the grid-cell that cannot sustain a fire, normalized from 0 % ($\text{Frag}_\text{n} = 0$) to 100 % ($\text{Frag}_\text{n} = 1$). Frag_exp is the shape parameter, determined through the optimization procedure.

Fire suppression is modeled as a function of land use (human presence), GDP, and fire intensity. This approach assumes that (1) fire suppression activities are limited in regions with low GDP and in remote areas with little land use, regardless of GDP (e.g. boreal fires in Canada and Alaska, bush fires in northern Australia); and (2) fire suppression efforts are less effective on more intense fires. These assumptions are embodied in the following equation:

$$\text{Supp}_\text{termp} = \left(1 - \left(1 - \text{LU}_\text{n}^{\text{LUSUPexp}}\right) \cdot \left(1 - \text{GDP}_\text{n}^{\text{GDPexp}}\right)\right) \cdot (1 - F_\text{intensity}) \tag{11}$$

where LU_n is the fraction of the grid-cell with land use, normalized from 0 ($\text{LU}_\text{n} = 0$) to 0.1 ($\text{LU}_\text{n} = 1$), LUSUP_exp a shape parameter controlling the increase in suppression effort with land use density, GDP_n is the normalized GDP (from 0 to 60 000$/capita), GDP_exp the shape parameter, and $F_\text{intensity}$ a proxy of fire intensity. LUSUP_exp and GDP_exp are determined through the optimization procedure. $F_\text{intensity}$ is dependent on weather conditions and fuel, assuming higher intensity with windier, drier, hotter conditions and with higher fuel load:

$$F_\text{intensity} = \left(1 - \text{RH}_\text{n}^{\text{RH}_\text{exp}}\right) \cdot \left(1 - \text{SW}_\text{n}^{\text{SW}_\text{exp}}\right) \cdot \left(1 - T_\text{n}^{T_\text{exp}}\right) \cdot G(W) \cdot \text{Precip}_\text{n}^{\text{FUELexp}} \tag{12}$$

2.3 Model optimization

The 9 optimized parameters (Table 1) are classified in 2 categories:

a. Non-shape parameters (2 out of 9) account for quantitative impacts of fire drivers: the default number of human ignitions per land use area (LUign), and the probability that lightning strikes on vegetated areas ignite a fire (CG_firep).

b. Shape parameters (7 out of 9) control the shape of the relationship between a given driver and fire. For example, relative humidity is assumed to limit fire spread between 30 % and 80 %, but the linear or non-linear relationship with relative humidity between 30 % and 80 % and fire spread is unclear. The shape parameter RH_{exp} (Eq. 4) is thus optimized and can convey a wide range of potential driving relationships (Fig. 2).

The exponential function for shape parameters was selected to balance gains in process understanding and costs associated with computational efforts. We assumed that fires respond monotonically to all optimized drivers, but acknowledge that more complex fire driving relationships cannot be accounted for here. Exploring such aspects would require 2 or more parameters per driver, which would lead to computational speed and convergence problems during optimization. The objective was to infer general conclusions on otherwise little understood fire drivers, for which single-parameter functions were well adapted.

We used a Markov Chain Monte Carlo approach based on the Metropolis Algorithm (Metropolis et al., 1953) to obtain best-fit parameter values. The algorithm generates trial sets of parameters pseudo-randomly, and compares model outputs with observational data. Each trial set is either accepted or rejected, and the history of acceptance and rejection guides the generation of subsequent trial sets. Acceptance occurs if a trial set leads to a better fit than the current parameterization. To limit the risk of convergence to local optimums, acceptance may also occur if the trial set does not have a better fit, with decreasing likelihood as the difference with the best fit increases. Upon acceptance (rejection), the range of possible parameter values is increased (decreased) before the next trial set is generated. The algorithm typically explored hundreds to over a thousand sets of trial parameter values before converging to a best fit (Fig. 3).

The optimization metric was defined to minimize classification error across 7 classes of annual burned fraction (interval boundaries: 0, 1, 5, 10, 20, 35, 50+% of the grid-

BGD
11, 10779–10826, 2014

cell), and to maximize the correlation with observed interannual variability:

$$\mathrm{Opt}_{\mathrm{index}} = \frac{\sum_{\mathrm{gridcell}\ =1}^{n}(\mathrm{MOD}_{\mathrm{fclass}} - \mathrm{OBS}_{\mathrm{class}})^2 + \sum_{\mathrm{gridcell}\ =1}^{n}(1 - \mathrm{IAV}_{\mathrm{correcoef}}(\mathrm{Mod},\ \mathrm{OBS}))}{n} \tag{13}$$

where $\mathrm{MOD}_{\mathrm{fclass}}$ and $\mathrm{OBS}_{\mathrm{class}}$ are the modeled and observed fire classification, and $\mathrm{IAV}_{\mathrm{correcoef}}$ the correlation coefficients for both time series, for each grid-cell.

The optimization was performed using modeled and observed burned area over 5 yr (2002–2007). Fewer than 2 % of all land grid-cells were used for the optimization step; these were selected manually to represent the broad spectrum of fire regimes and the range of environmental conditions around the world (e.g. biomes, land use density, fuel gradient in semi-arid regions, GDP). No grid-cells were selected from South America, in order to test the model's ability to reproduce fire patterns under combinations of drivers it might not have encountered during optimization. To evaluate the robustness of the algorithm convergence, we performed 20 optimization runs, each using different grid-cells and years. The algorithm was a very valuable tool applied repeatedly throughout model development to support its design. In particular, we used it to test the relevancy of additional fire driving mechanisms by quantifying the gain in the optimization index, to progressively adapt non-optimized parameters (e.g. input normalization range), and to compare the performance with different data sources (e.g. alternative land cover datasets).

2.3.1 Model evaluation

We evaluated HESFIRE using satellite-derived estimates of (1) burned area and aggregate characteristics of regional fire activity over a 13-years timespan (fire incidence, seasonality, interannual variability); and (2) the regional distribution of fire size for the year 2005.

Finally, we performed a sensitivity analysis to evaluate the influence of each model parameter on the averaged annual burned area within the model. For each parameter, the model was run twice, with the parameter changed to +50 % and -50 % of its original value while everything else was kept the same. For each grid-cell, we then extracted the parameter that generated the largest change in burned area. Results of the sensitivity analysis were grouped into four classes to map the spatial distribution of parameter sensitivity: (1) climate (lightning strike, RH, soil moisture and temperature parameters); (2) fuel (precipitation-based proxy); (3) anthropogenic (ignitions and suppression parameters); (4) fragmentation (landscape fragmentation parameter).

2.4 Data

2.4.1 Weather

We combined two data sources to estimate the spatial and temporal variability in natural ignitions from lightning. The timing and location of cloud-to-ground lightning strikes is based on convective precipitation (Allen and Pickering, 2002) using sub-daily convective precipitation data from NCEP (see below). We then corrected biases in the spatial distribution of lightning strikes identified by the authors of this method with the observed LIS/OTD climatology (Christian et al., 2003), converted to cloud-to-ground lightning strikes only following Prentice and Mackerras (1977).

Sub-daily relative humidity, soil moisture, temperature, wind speed and convective precipitation data were obtained from the NCEP reanalysis-II project (Kanamitsu et al., 2002). For fuel limitation, we used monthly precipitation data from the Global Precipitation Climatology Project (GPCP, Adler et al., 2003). All data were interpolated linearly from their original resolution (2.5° for NCEP) to the model 1° resolution, and averaged from 6-hourly to 12-hourly.

2.4.2 Land cover

We used the GlobCover version 2.3 land cover map (Bontemps et al., 2011) to estimate the distribution of natural ecosystems and human land uses at 1° resolution. GlobCover

BGD
11, 10779–10826, 2014
HESFIRE
Y. Le Page et al.

data were re-gridded from the original 300 m resolution to 1° and reclassified from 22 land cover classes to the 5 classes used in the model (forests, shrublands, grasslands, croplands/urban, bare areas/water).

2.4.3 Land use and GDP

Land use density was computed as the sum of crops and urban lands in the GlobCover data. National GDP was inferred from the 2009 World Factbook (CIA, 2009).

2.4.4 Fire activity

The Global Fire Emission Database (GFED version 3, van der Werf et al., 2010) was used in the optimization procedure as well as to evaluate the representation of fire incidence, seasonality and interannual variability in HESFIRE. The regional distribution of fire was evaluated with observations from the MODIS MCD45 burned area product (Roy et al., 2008).

3 Results

3.1 Optimization

The parameters inferred by the optimization procedure are consistent with our current understanding of fire drivers, and provide a quantitative estimate on otherwise poorly constrained relationships. Their value, variability across the 20 optimization runs and implications for fire ignition, spread and termination are presented in Figs. 4 and 5. In 16 out of the 20 optimization runs performed, the final set of parameters was relatively similar to the final model, and changes in parameter values were mostly compensative of each other, especially for correlated fire drivers (e.g. relative humidity and soil moisture). In four cases, the optimization procedure reached an alternative configuration, with one or several parameters differing from the final parameterization by a factor

BGD
11, 10779–10826, 2014

greater than five, and were discarded as unsuccessful parameterization, most likely getting stuck at local optimums. Hereafter, we refer to the remaining 16 models to consider parameter uncertainty, represented by the black lines in Fig. 4 and shaded areas in Fig. 5.

For fire ignitions, the probability that lightning strikes on natural vegetation ignite a fire under fire prone conditions is optimized at 6.8 % (uncertainty range [2.8 to 16.6 %]), comparable to the value inferred from the literature used in SPITFIRE (4 %, Thonicke et al., 2010). We emphasize, however, that this metric is a general probability which does not depict the complex relationship between cloud-to-ground lightning strikes and fire ignitions (Podur et al., 2003). Regarding anthropogenic sources, the optimization procedure suggests that ignition-saturated fire regimes (Knorr et al., 2013) are very common in landscapes with human activities, with any additional land use beyond 2–3 % of the grid-cell area having no contribution to ignitions (Fig. 5a). The final number of anthropogenic ignitions further depends on GDP per capita, with a nearly linear relationship Fig. 5b.

Regarding fire spread, exponents depicting the role of RH and soil moisture indicate relatively linear relationships, with significant uncertainty (RHexp = 1.18 [0.52 to 1.29]; SWexp = 1.21 [0.3 to 1.44]) (Fig. 5d and e). The relationship with temperature is slightly non-linear (Texp = 1.78 [0.80 to 3.30]), indicating a lower impact of temperature changes towards the higher range of the influence interval ([0 30 °C]). Optimizing the model without the influence of temperature produced relatively similar performance, except in high-latitude regions where temperature constraints encompass limits on fire spread (e.g., snow cover).

For fire termination, the anthropogenic influence indicated a rapid saturation of suppression efforts with land use density (LUSUPexp = 4.08 [1.62 to 7.18]) and maximum suppression at 0.1 fractional land use (Fig. 5a). The influence of GDP was approximately linear (GDPexp = 1.28 [0.97 to 2.24]), while the influence of landscape fragmentation was slightly non-linear (FRAGexp = 1.41 [0.83 to 3.02]). Note that a substantial amount of landscape fragmentation is due to human activities, adding to the anthropogenic footprint on fire activity. The cumulative precipitation proxy for fuel load also indicated a slightly non-linear relationship (FUELexp = 1.72 [1.62 to 3.65]). Climatic factors only operate through condition thresholds (e.g. relative humidity over 80 %) and were thus not optimized.

3.2 Global 1997–2010 run and comparison to observation-derived data

The modeled and observed average annual burned fractions across the world are illustrated in Fig. 6. In South America, which was not part of the optimization phase, HESFIRE depicts most spatial patterns as well as the actual incidence of fires, including increased fire activity associated with the expansion of human activities into the Amazon basin, the competing influence of the moisture gradient, and fires associated with pastures and grasslands in northern Venezuela and southern Columbia. HESFIRE generally captures high fire incidence regions in grasslands of Africa and Australia, although modeled spatial patterns of fire activity in Africa are more uniform than observations. It also reproduces areas of moderate fire incidence in south-eastern Asia, Kazakhstan and south-western Europe, and identifies strong fire gradients with decreasing fuel load across semi-arid and arid regions (e.g. in Africa, central Australia), although with some limitation especially at the northern edge of sub-Saharan Africa where fire incidence is over-estimated. Conversely, HESFIRE performs poorly in several regions, including the pan-boreal region, at least partly due to a bias in the climate and soil moisture data (see discussion), as well as Central America, Mexico, the horn of Africa and some areas of the Middle East where fire incidence is over-estimated. It also under-estimates fire incidence in Indonesia, where soil moisture remains beyond the fire prone threshold almost all year long. Fires preferentially occur on areas with degraded forests and drained peatlands in Indonesia (Page et al., 2002; Van der Werf et al., 2008), which moisture dynamics is not captured in a 2.5° resolution dataset.

Aggregated monthly burned area across 14 regions and their respective fire size distribution are illustrated in Fig. 7. The monthly time series provide insights into the performance of HESFIRE on regional fire incidence, fire seasonality and inter-annual variability. Average burned area in the main fire incidence regions are in agreement with the GFED database (NHAF, SHAF, AUST, SHSA). Seasonality also shows a good agreement, whether regionally or at 1° resolution (not shown). The main seasonality discrepancy occurs in sub-Saharan Africa, where the model substantially delays the onset and peak of the fire season. Finally, HESFIRE performs unevenly regarding inter-annual variability, with medium to high correlation to observations in tropical and temperate regions, but low or even negative correlation in boreal regions. It reproduces the El Nino induced anomaly in Indonesia in 1997–1998, but because of the underestimation of fire incidence mentioned before, the actual extent of that extreme fire episode is not captured.

Next to each time series, the regional fire size distribution histograms suggest the representation of single fire size in HESFIRE is within the range of observations, and that it depicts the decreasing fire frequency as a function of fire size. It tends to overestimate the frequency of large fires and their contribution to the total burned area, however. 68 % of the 2005 burned area occurred in fires longer than one day in HESFIRE, which could not be readily evaluated with the MODIS data.

3.3 Model sensitivity

The sensitivity analysis shows the class of the parameter whose altered values (+50 % and −50 %) led to the largest change in averaged annual burned area at the grid-cell level (Fig. 8). In boreal regions, although HESFIRE does not perform well, fire incidence is mostly sensitive to weather parameters, and to a lower extent to the fuel load parameter. In humid tropical ecosystems, HESFIRE is also mostly sensitive to weather parameters, but anthropogenic parameters become dominant in areas with a substantial dry season and agricultural activities, especially in South America along the arc of deforestation. In semi-arid areas, the vegetation fuel parameter has the most influence, including in Mexico, sub-Saharan and southern sub-equatorial Africa, the horn of Africa, Australia and Kazakhstan, with consequences for the model performance in these various regions (see discussion). Finally, HESFIRE is primarily sensitive to

BGD
11, 10779–10826, 2014

the landscape fragmentation parameter in several regions due to two mechanisms. In regions of high land use density (e.g. India), fire spread is constantly limited by the fragmentation parameter and fire incidence is low, but can increase (or diminish further) when altering its value. In regions of low land use density but high fire incidence due to a very seasonal climatology (e.g. sub-Saharan and northern sub-equatorial Africa), landscape fragmentation due to previous fires becomes a limiting factor for late-season fires. Finally, regions of relatively high land use density and fire incidence are probably sensitive to both mechanisms.

4 Discussion

4.1 Model performance and potential improvements

HESFIRE shows encouraging capabilities, especially given the difficulty of achieving a good representation of global fire patterns (Bowman et al., 2011; Spessa et al., 2013). It is a first step towards the 3 objectives stated in introduction. First, the model avoids some assumptions that would be fundamentally inconsistent with fire ecology (e.g. fire spread limited to a single day). Second, it includes climatic, anthropogenic and vegetation drivers, and the input variables were chosen so as to enable integration within dynamic vegetation and integrated assessment models (e.g. human ignitions dependent on land use instead of population). Third, HESFIRE reproduces reasonably well many aspects of regional fire activity, including fire incidence and variability in South America and fire size, both of which were not part of the optimization procedure, and its regional sensitivity to the 4 parameter classes corresponds to what would be expected based on broad fire ecology concepts.

The comparison to results reported by other models – mostly fire incidence – suggests HESFIRE generally achieves strong performances on spatial patterns (Fig. 6 in this paper, Fig. 3c in Thonicke et al., 2010, Fig. 2 in Prentice et al., 2011, Fig. 1 in Kloster et al., 2010), and on the actual quantification of the average burned area fraction, with a rather infrequent occurrence of large discrepancies which are susceptible to severely bias impacts on vegetation and carbon dynamics. Note however that these results are not fully comparable as they are produced from fire-modules embedded within dynamic vegetation models, with potential bias originating from other parts of the model (e.g. land cover, fuel load). The fire model developed by (Li et al., 2012) and modified to better account for anthropogenic ignitions has similar spatial patterns of averaged burned area to HESFIRE (Fig. 9 in Li et al., 2013a).

The combination of these characteristics and performance suggests that the modeling and optimization framework realistically captures the primary fire-driving mechanisms and the specific magnitude of their influence regionally. It could thus bring relevant insights into future fire activity under altered environmental conditions, including agricultural expansion and extreme climatic events (e.g. sustained droughts). There are however a number of issues, as well as key potential improvements which we discuss in the next sections.

4.1.1 Fire incidence in boreal regions

HESFIRE under-estimates fire incidence in Boreal regions. This issue has been reported before by Rupp et al. (2007), whose model projected almost no burned area when driven by the NCEP data but performed better when driven by other datasets. (Serreze and Hurst, 2000) found that summer precipitation is largely over-estimated in NCEP, compromising the whole hydrological cycle including RH and soil moisture. Alternative datasets may address this issue (e.g. for RH: MERRA, Rienecker et al., 2011; AIRS, Fetzer et al., 2003), either by using them as a direct input or to correct the bias in the NCEP data while maintaining its high temporal resolution and extensive timespan.

HESFIRE might be further limited because it does not represent specific aspects of boreal fire regimes. In particular, boreal needle-leaf forests are highly flammable and have a vertical structure favorable to the development of crown fires, which spread faster and can overcome higher levels of moisture and humidity (Ryan, 2002). Additionally, large boreal fires typically spread over weeks or months – which can be captured

BGD
11, 10779–10826, 2014

by HESFIRE – but might also remain dormant in a smoldering phase during fire-averse conditions and re-activate later without any new ignitions (Sedano and Randerson, 2014).

4.1.2 Fires in semi-arid regions and links to the fuel proxy

Semi-arid ecosystems presented a particular challenge due to the sensitivity of fuel characteristics to soil, precipitation and potential evapotranspiration conditions, which cannot be fully captured by the cumulative precipitation proxy. In the final parameterization, HESFIRE is in good agreement with observations in Australia, Southern Hemisphere Africa and Kazakhstan, but over-estimates fire incidence in Mexico, the horn of Africa and semi-desert areas at the border of the Sahara (Fig. 8). Precipitation patterns in these xeric landscapes vary widely. Some semi-desert regions have low amounts of precipitation year-round (Kazakhstan), while others have short rainy seasons (sub-Saharan Africa). The optimization procedure favors one set of conditions, leading to unequal performances across these regions.

Clearly there are other potential factors contributing to this issue, but most of them are likely related to fuel characteristics. The integration of HESFIRE within a vegetation model (Sect. 4.2.3) will be important to provide dynamic and process-based estimates of fuel load, fuel structure and fuel moisture (see Sect 4.2.3). In parallel, integrating observation-derived estimates of aboveground biomass (Saatchi et al., 2011) as a fuel-proxy could improve performances while maintaining the value of a standalone version of HESFIRE.

4.1.3 Representation of anthropogenic ignitions

Modeling the global diversity of anthropogenic fire practices remains a significant challenge. HESFIRE performs well in regions with a well-established anthropogenic footprint on fire regimes, even though it is based on a simplistic representation of fire practices and suppression effort by necessity to obtain a globally consistent initial approach.

BGD
11, 10779–10826, 2014
HESFIRE
Y. Le Page et al.

The timing and frequency of anthropogenic ignitions are a complex aspect to represent in global models. In sub-Saharan Africa for example, local populations are known to burn numerous small fires early in the dry season to fragment the landscape and limit the occurrence of high-intensity late-season fires (Laris, 2002; Le Page et al., 2010a). These fire management practices are not accounted for in HESFIRE, leading to a delayed fire-peak month (by 1–3 months), and to an over-estimation of the average fire size. Beyond this specific case, fire practices vary as a function of land use (e.g. agriculture, pastures), of land use transitions (e.g. deforestation and post-clearing activities Morton et al. (2008), of land management practices (fire prevention, fire suppression), and can also be due to arson or leisure activities (e.g. campfire). For agricultural lands, fire practices can be very specific (clearing, pre-sowing, pre- and post-harvest burns) and last for as little as a week to several months (Le Page et al., 2010a). Finally, these practices vary at local to global scale according to environmental conditions, the availability of alternatives to fires (e.g. fertilizer, pest control), national regulations, fire fighting capabilities, etc. This cannot nearly be accounted for in a global model designed to be used for future projection, but a future version of HESFIRE will represent broad classes of fire practices separately (agricultural, deforestation/shifting cultivation and management fires), leveraging the approach developed in Li et al. (2013b).

4.1.4 Representation of fire spread

The evaluation suggests the modeled average fire size is within the observed range, but HESFIRE tends to overestimate the contribution of large fires, which could be linked to the representation of fire spread as an idealized elliptic shape, and to the simple accounting of anthropogenic ignitions. Burned areas are typically patchy and the front line rarely remains unbroken around the perimeter of the fire, especially in fragmented and uneven landscapes. Adopting a strategy to better account for these characteristics will be tested with the implementation of a fragmentation feedback on the fraction of the idealized elliptical shape that actually burns.

BGD
11, 10779–10826, 2014

Additionally, anthropogenic fire practices mentioned in Sect. 4.1.3 can have a substantial footprint on fire size, including in regions where it is over-estimated by HESFIRE. In sub-Saharan Africa for example, plans to explicitly represent small early dry-season burns as a fire management practice should lead to a more realistic accounting of fire sizes and of the landscape fragmentation feedback on late-season fire spread. Accordingly, we also plan to revisit the definition of the fragmentation index, using an approach accounting for intra-grid-cell patchiness (e.g. Jaeger, 2000; Schumaker, 1996).

4.2 Applications to environmental issues and for decision support

4.2.1 Projection of future fire activity

Large scale policy decisions on agricultural production and climate mitigation will have impacts on fire activity and might have to adapt in response, which HESFIRE could help anticipate. Projections of agricultural lands point to a wide range of potential outcomes regarding their expansion in natural ecosystems, depending among other factors on food demand, technological developments and policies such as incentives for forest conservation (e.g. REDD) or biofuels expansion (DeFries and Rosenzweig, 2010; Thomson et al., 2010; Tilman et al., 2011). Given the sensitivity of fire activity to human presence in the landscape and to climate, it is essential to anticipate the fire impacts of these scenarios, as well as the synergies and trade-offs with their respective societal goals (e.g. climate mitigation, food security, biodiversity). An integrated perspective is key to understand the interactions in play and to provide some level of confidence in projections of fire regimes under altered environmental conditions (Bowman et al., 2009, 2011). We believe HESFIRE as a standalone version can provide relevant insights on fire incidence and variability under projections of future climate (Taylor et al., 2012), land use (Hurtt et al., 2011) and societal conditions (Van Vuuren et al., 2011), and on regional sensitivities to the potential magnitude of these changes.

BGD
11, 10779–10826, 2014

4.2.2 Regional versions of the model

The development of regional HESFIRE versions has significant potential, and we are particularly interested in such collaborations. The optimization procedure can be applied to any spatial subset to better capture specific regional interactions, especially regarding fire practices, fuel dynamics and climatic influence, for which global parameters imply substantial regional tradeoffs (Sect. 4.1.2 and 4.1.3). Replacing global input data with high quality regional data (e.g. land cover) is straightforward in HESFIRE, and regional versions could support the development of new capabilities (e.g. disaggregation of the forest class into needle-leaved and broad-leaved forests with specific fire parameters).

4.2.3 Integration to vegetation and socio-economic models

Beyond fire incidence and variability, fire impacts are of primary importance in multiple contexts, including climate mitigation policies and the global carbon cycle (Le Page et al., 2013; van der Werf et al., 2010), ecosystem dynamics across major biomes (Bond-Lamberty et al., 2007; Cochrane, 2009), as well as pollution, health effects and a wide range of economic aspects (e.g. Bowman et al., 2011; Calkin et al., 2005; Kochi et al., 2010; Sastry, 2002). Exploring these issues requires key developments of the fire-modeling framework.

First, impacts on ecosystem dynamics, the carbon cycle and other pollutant emissions need to be developed within a dynamic vegetation model. Again, we will benefit from previous work regarding ecosystem impacts and emissions (e.g. Thonicke et al., 2010). HESFIRE is being implemented in the Ecosystem Demography model (ED, Moorcroft et al., 2001) and has to be adapted to the new fuel capabilities, and for fire impacts. Parameters will have to be optimized again, which is not an issue given the computational efficiency of the ED model and the optimization performance on a small subset of the spatial domain. The ED model is particularly well adapted for fire impacts modeling because it tracks vegetation patches of different ages within a grid-cell and the size and type of successional cohorts within each patch. Such characteristics will be essential to realistically estimate fire behavior (e.g. ladder fuel and crown vs. understory fires), fire intensity and combustion completeness, size and PFT dependent fire-induced mortality (Brando et al., 2012), snags and downed-fuel decomposition rates (Chambers et al., 2000; Palace et al., 2008), and post-fire regrowth dynamics (Balch et al., 2008; Bond-Lamberty et al., 2007; Goetz et al., 2007).

Second, the role of fires within the Human–Earth system needs to be explored within an integrated framework to provide consistent scenarios of climate, ecosystems and society under different environmental policy assumptions (Le Page et al., 2013). HESFIRE has been specifically developed to this end, with anthropogenic input data commonly reported and projected by integrated assessment models (land use and GDP). Recent developments to couple integrated assessment models to process-based vegetation and climate models (Jones et al., 2013) enable the simultaneous consideration of societal, vegetation and climate dynamics and how they feed back on each other, without the need to exogenously specify input data from other models run under potentially conflicting assumptions and forcing. Such a framework is particularly relevant to explore fires and their interaction within the Human–Earth System.

5 Conclusions

HESFIRE and its optimization procedure provide a relevant tool to explore certain aspects of fire ecology and to anticipate potential changes in fire activity. We provide a first assessment of the uncertainties attached to the parameters and the model sensitivity to the driving assumptions they represent. We identify limitations and propose key developments to address the most significant ones. Finally, we propose applications of HESFIRE, as a standalone version or with its implementation into other frameworks to contribute to a better understanding of contemporary and future fire activity, to support estimates of greenhouse gas emissions and ecosystem dynamics, and to provide

BGD
11, 10779–10826, 2014
HESFIRE
Y. Le Page et al.

policy makers with insights into the consequences of potential economic and environmental decisions.

Author contribution

Y. L. P. developed the model and performed the simulations, Y. L. P., B. B. L. and G. H. designed the optimization procedure, Y.L.P. prepared the manuscript with contribution from all authors.

Acknowledgements. The authors are grateful for research support provided by the NASA Terrestrial Ecology and Inter-Disciplinary Studies programs. The authors also wish to express appreciation to the Integrated Assessment Research Program in the Office of Science of the US Department of Energy for partially funding this research. The Pacific Northwest National Laboratory is operated for DOE by Battelle Memorial Institute under contract DE-AC05- 76RL01830. The views and opinions expressed in this paper are those of the authors alone.

References

Abatzoglou, J. T. and Kolden, C. A.: Relative importance of weather and climate on wildfire growth in interior Alaska, Int. J. Wildland Fire, 20, 79–486, 2011.

Adler, R. F., Huffman, G. J., Chang, A., Ferraro, R., Xie, P. P., Janowiak, J., Rudolf, B., Schneider, U., Curtis, S., and Bolvin, D.: The version-2 global precipitation climatology project (GPCP) monthly precipitation analysis (1979-present), J. Hydrometeorol., 4, 1147–1167, 2003.

Allen, D. J. and Pickering, K. E.: Evaluation of lightning flash rate parameterizations for use in a global chemical transport model, J. Geophys. Res.-Atmos. (1984–2012), 107, G02008, doi:10.1029/2005JG000042, 2002.

Arora, V. K. and Boer, G. J.: Fire as an interactive component of dynamic vegetation models, available at: http://www.agu.org/journals/jg/jg0504/2005JG000042/2005jg000042-t01.txt (last access: 5 June 2013), J. Geophys. Res.-Biogeo. (2005–2012), 110, G02008, doi:10.1029/2005JG000042, 2005.

BGD
11, 10779–10826, 2014
HESFIRE
Y. Le Page et al.

Balch, J. K., Nepstad, D. C., Brando, P. M., Curran, L. M., Portela, O., de Carvalho, O., and Lefebvre, P.: Negative fire feedback in a transitional forest of southeastern Amazonia, Glob. Change Biol., 14, 2276–2287, 2008.
Bond-Lamberty, B., Peckham, S. D., Ahl, D. E., and Gower, S. T.: Fire as the dominant driver of central Canadian boreal forest carbon balance, Nature, 450, 89–92, 2007.
Bontemps, S., Defourny, P., Bogaert, E. V., Arino, O., Kalogirou, V., and Perez, J. R.: GLOBCOVER 2009 – Products Description and Validation Report, available at: http://www.citeulike.org/group/15400/article/12770349 (last access: 25 February 2014), 2011.
Bowman, D. M. J. S., Balch, J. K., Artaxo, P., Bond, W. J., Carlson, J. M., Cochrane, M. A., D'Antonio, C. M., DeFries, R. S., Doyle, J. C., Harrison, S. P., Johnston, F. H., Keeley, J. E., Krawchuk, M. A., Kull, C. A., Marston, J. B., Moritz, M. A., Prentice, I. C., Roos, C. I., Scott, A. C., Swetnam, T. W., van der Werf, G. R., and Pyne, S. J.: Fire in the Earth System, Science, 324, 481–484, doi:10.1126/science.1163886, 2009.
Bowman, D. M. J. S., Balch, J., Artaxo, P., Bond, W. J., Cochrane, M. A., D'Antonio, C. M., DeFries, R., Johnston, F. H., Keeley, J. E., Krawchuk, M. A., Kull, C. A., Mack, M., Moritz, M. A., Pyne, S., Roos, C. I., Scott, A. C., Sodhi, N. S., and Swetnam, T. W.: The human dimension of fire regimes on Earth, J. Biogeogr., 38, 2223–2236, doi:10.1111/j.1365-2699.2011.02595.x, 2011.
Brando, P. M., Nepstad, D. C., Balch, J. K., Bolker, B., Christman, M. C., Coe, M., and Putz, F. E.: Fire-induced tree mortality in a neotropical forest: the roles of bark traits, tree size, wood density and fire behavior, Glob. Change Biol., 18, 630–641, 2012.
Calkin, D. E., Gebert, K. M., Jones, J. G., and Neilson, R. P.: Forest service large fire area burned and suppression expenditure trends, 1970–2002, available at: http://www.fs.fed.us/pnw/pubs/journals/pnw_2005_calkin001.pdf, (last access 17 April 2014), 2005.
Cardoso, M. F., Hurtt, G. C., Moore, B., Nobre, C. A., and Prins, E. M.: Projecting future fire activity in Amazonia, Glob. Change Biol., 9, 656–669, 2003.
Chambers, J. Q., Higuchi, N., Schimel, J. P., Ferreira, L. V., and Melack, J. M.: Decomposition and carbon cycling of dead trees in tropical forests of the central Amazon, Oecologia, 122, 380–388, 2000.
CIA, E.: The World Factbook 2009, [online] available at: https://www.cia.gov/library/publications/download/download-2009, Central Intelligence Agency, Washington, DC, 2009.
Cochrane, M. A.: Tropical Fire Ecology, Fire, Land Use, Land Cover Dynamics, and Climate Change in the Brazilian Amazon, 389–426, 2009.

Cramer, W., Bondeau, A., Woodward, F. I., Prentice, I. C., Betts, R. A., Brovkin, V., Cox, P. M., Fisher, V., Foley, J. A., and Friend, A. D.: Global response of terrestrial ecosystem structure and function to CO_2 and climate change: results from six dynamic global vegetation models, Glob. Change Biol., 7, 357–373, 2001.

DeFries, R. and Rosenzweig, C.: Toward a whole-landscape approach for sustainable land use in the tropics, P. Natl. Acad. Sci. USA, 107, 19627–19632, doi:10.1073/pnas.1011163107, 2010.

Fetzer, E., McMillin, L. M., Tobin, D., Aumann, H. H., Gunson, M. R., McMillan, W. W., Hagan, D. E., Hofstadter, M. D., Yoe, J., and Whiteman, D. N.: Airs/amsu/hsb validation, IEEE T. Geosci. Remote, 41, 418–431, 2003.

Flannigan, M., Stocks, B., Turetsky, M., and Wotton, M.: Impacts of climate change on fire activity and fire management in the circumboreal forest, Glob. Change Biol., 15, 549–560, doi:10.1111/j.1365-2486.2008.01660.x, 2009.

Gillett, N. P., Weaver, A. J., Zwiers, F. W., and Flannigan, M. D.: Detecting the effect of climate change on Canadian forest fires, Geophys. Res. Lett., 31, L18211, doi:10.1029/2004GL020876, 2004.

Goetz, S. J., Bunn, A. G., Fiske, G. J., and Houghton, R. A.: Satellite-observed photosynthetic trends across boreal North America associated with climate and fire disturbance, P. Natl. Acad. Sci. USA, 102, 13521–13525, 2005.

Goetz, S. J., Mack, M. C., Gurney, K. R., Randerson, J. T., and Houghton, R. A.: Ecosystem responses to recent climate change and fire disturbance at northern high latitudes: observations and model results contrasting northern Eurasia and North America, Environ. Res. Lett., 2, 045031, doi:10.1088/1748-9326/2/4/045031, 2007.

Hurtt, G., Chini, L., Frolking, S., Betts, R., Feddema, J., Fischer, G., Fisk, J., Hibbard, K., Houghton, R., Janetos, A., Jones, C. D., Kindermann, G., Kinoshita, T., Goldewijk, K. K., Riahi, K., Shevliakova, E., Smith, S., Stehfest, E., Thomson, A., Thornton, P., van Vuuren, D. P., and Wang, Y. P.: Harmonization of land-use scenarios for the period 1500–2100: 600 years of global gridded annual land-use transitions, wood harvest, and resulting secondary lands, Climatic Change, 109, 1–45, 2011.

Jaeger, J. A.: Landscape division, splitting index, and effective mesh size: new measures of landscape fragmentation, Landscape Ecol., 15, 115–130, 2000.

Jones, A. D., Collins, W. D., Edmonds, J., Torn, M. S., Janetos, A., Calvin, K. V., Thomson, A., Chini, L. P., Mao, J., and Shi, X.: Greenhouse gas policy influences climate via direct effects of land-use change, J. Climate, 26, 3657–3670, 2013.

Kanamitsu, M., Ebisuzaki, W., Woollen, J., Yang, S. K., Hnilo, J. J., Fiorino, M., and Potter, G. L.: Ncep-doe amip-ii reanalysis (r-2), B. Am. Meteorol. Soc., 83, 1631–1644, 2002.

Keeley, J. E. and Fotheringham, C. J.: Impact of past, present, and future fire regimes on North American Mediterranean shrublands, in: Fire and Climatic Change in Temperate Ecosystems of the Western Americas, Springer, 218–262, available at: http://link.springer.com/chapter/10.1007/0-387-21710-X_8 (last access: 5 June 2013), 2003.

Kloster, S., Mahowald, N. M., Randerson, J. T., Thornton, P. E., Hoffman, F. M., Levis, S., Lawrence, P. J., Feddema, J. J., Oleson, K. W., and Lawrence, D. M.: Fire dynamics during the 20th century simulated by the Community Land Model, Biogeosciences, 7, 1877–1902, doi:10.5194/bg-7-1877-2010, 2010.

Kloster, S., Mahowald, N. M., Randerson, J. T., and Lawrence, P. J.: The impacts of climate, land use, and demography on fires during the 21st century simulated by CLM-CN, Biogeosciences, 9, 509–525, doi:10.5194/bg-9-509-2012, 2012.

Knorr, W., Kaminski, T., Arneth, A., and Weber, U.: Impact of human population density on fire frequency at the global scale, Biogeosciences, 11, 1085–1102, doi:10.5194/bg-11-1085-2014, 2014.

Kochi, I., Donovan, G. H., Champ, P. A., and Loomis, J. B.: The economic cost of adverse health effectsfrom wildfire-smoke exposure: a review, Int. J. Wildland Fire, 19, 803–817, 2010.

Korontzi, S., McCarty, J., Loboda, T., Kumar, S., and Justice, C.: Global distribution of agricultural fires in croplands from 3 years of Moderate Resolution Imaging Spectroradiometer (MODIS) data, Global Biogeochem. Cy., 20, GB2021, doi:10.1029/2005GB002529, 2006.

Laris, P.: Burning the seasonal mosaic: preventative burning strategies in the wooded savanna of southern Mali, Hum. Ecol., 30, 155–186, 2002.

Le Page, Y., Pereira, J. M. C., Trigo, R., da Camara, C., Oom, D., and Mota, B.: Global fire activity patterns (1996–2006) and climatic influence: an analysis using the World Fire Atlas, Atmos. Chem. Phys., 8, 1911–1924, doi:10.5194/acp-8-1911-2008, 2008.

Le Page, Y., Oom, D., Silva, J., Jönsson, P., and Pereira, J.: Seasonality of vegetation fires as modified by human action: observing the deviation from eco-climatic fire regimes, Global Ecol. Biogeogr., 19, 575–588, 2010a.

Le Page, Y., van der Werf, G., Morton, D., and Pereira, J.: Modeling fire-driven deforestation potential in Amazonia under current and projected climate conditions, J. Geophys. Res., 115, G03012, doi:10.1029/2009JG001190, 2010b.
Le Page, Y., Hurtt, G., Thomson, A. M., Bond-Lamberty, B., Patel, P., Wise, M., Calvin, K., Kyle, P., Clarke, L., Edmonds, J., and Janetos, A.: Sensitivity of climat mitigation strategies to natural disturbances, Environ. Res. Lett., 8, 015018, doi:10.1088/1748-9326/8/1/015018, 2013.

Li, F., Zeng, X. D., and Levis, S.: A process-based fire parameterization of intermediate complexity in a Dynamic Global Vegetation Model, Biogeosciences, 9, 2761–2780, doi:10.5194/bg-9-2761-2012, 2012.
Li, F., Levis, S., and Ward, D. S.: Quantifying the role of fire in the Earth system – Part 1: Improved global fire modeling in the Community Earth System Model (CESM1), Biogeosciences, 10, 2293–2314, doi:10.5194/bg-10-2293-2013, 2013a.
Li, F., Levis, S., and Ward, D. S.: Quantifying the role of fire in the Earth system – Part 1: Improved global fire modeling in the Community Earth System Model (CESM1), Biogeosciences, 10, 2293–2314, doi:10.5194/bg-10-2293-2013, 2013b.
Liu, Y., Stanturf, J., and Goodrick, S.: Trends in global wildfire potential in a changing climate, Forest Ecol. Manag., 259, 685–697, 2010.
Liu, Y., Goodrick, S., and Heilman, W.: Wildland fire emissions, carbon, and climate: wildfire–climate interactions, Forest Ecol. Manag., available at: http://www.sciencedirect.com/science/article/pii/S037811271300114X (last access: 28 February 2014), 317, 80–96, 2013.
Metropolis, N., Rosenbluth, A. W., Rosenbluth, M. N., Teller, A. H., and Teller, E.: Equation of state calculations by fast computing machines, J. Chem. Phys., 21, doi:10.1063/1.1699114, 1953.
Moorcroft, P., Hurtt, G., and Pacala, S.: A method for scaling vegetation dynamics: the ecosystem demography model (ED), Ecol. Monogr., 71, 557–586, 2001.
Morton, D. C., Defries, R. S., Randerson, J. T., Giglio, L., Schroeder, W., and van Der Werf, G. R.: Agricultural intensification increases deforestation fire activity in Amazonia, Glob. Change Biol., 14, 2262–2275, 2008.
Morton, D. C., Le Page, Y., DeFries, R., Collatz, G. J., and Hurtt, G. C.: Understorey fire frequency and the fate of burned forests in southern Amazonia, available at: http://rstb.

royalsocietypublishing.org/content/368/1619/20120163.short (last access: 7 October 2013), Philos. T. R. Soc. B, 368, doi:10.1098/rstb.2012.0163, 2013.
Mouillot, F., Schultz, M. G., Yue, C., Cadule, P., Tansey, K., Ciais, P., and Chuvieco, E.: Ten years of global burned area products from spaceborne remote sensing – a review: analysis of user needs and recommendations for future developments, Int. J. Appl. Earth Obs., 26, 64–79, doi:10.1016/j.jag.2013.05.014, 2014.
Page, S. E., Siegert, F., Rieley, J. O., Boehm, H.-D. V., Jaya, A., and Limin, S.: The amount of carbon released from peat and forest fires in Indonesia during 1997, Nature, 420, 61–65, 2002.
Palace, M., Keller, M., and Silva, H.: Necromass production: studies in undisturbed and logged Amazon forests, Ecol. Appl., 18, 873–884, 2008.
Parry, M. L.: Climate Change 2007: Impacts, Adaptation and Vulnerability: Working Group II Contribution to the Fourth Assessment Report of the IPCC Intergovernmental Panel on Climate Change, Cambridge University Press, available at: (last access: 25 September 2013), 2007.
Pechony, O. and Shindell, D. T.: Fire parameterization on a global scale, J. Geophys. Res.-Atmos. (1984–2012), 114, D16115, doi:10.1029/2009JD011927, 2009.
Pereira, M. G., Trigo, R. M., da Camara, C. C., Pereira, J. M. C., and Leite, S. M.: Synoptic patterns associated with large summer forest fires in Portugal, Agr. Forest Meteorol., 129, 11–25, doi:10.1016/j.agrformet.2004.12.007, 2005.
Pfeiffer, M., Spessa, A., and Kaplan, J. O.: A model for global biomass burning in preindustrial time: LPJ-LMfire (v1.0), Geosci. Model Dev., 6, 643–685, doi:10.5194/gmd-6-643-2013, 2013.
Podur, J., Martell, D. L., and Csillag, F.: Spatial patterns of lightning-caused forest fires in Ontario, 1976–1998, Ecol. Model., 164, 1–20, doi:10.1016/S0304-3800(02)00386-1, 2003.
Prentice, I. C., Kelley, D. I., Foster, P. N., Friedlingstein, P., Harrison, S. P., and Bartlein, P. J.: Modeling fire and the terrestrial carbon balance, Global Biogeochem. Cy., 25, GB3005, doi:10.1029/2010GB003906, 2011.
Prentice, S. A. and Mackerras, D.: The ratio of cloud to cloud-ground lightning flashes in thunderstorms, J. Appl. Meteorol., 16, 545–550, 1977.
Randerson, J. T., Liu, H., Flanner, M. G., Chambers, S. D., Jin, Y., Hess, P. G., Pfister, G., Mack, M. C., Treseder, K. K., Welp, L. R., Chapin, F. S., Harden, J. W., Goulden, M. L., Lyons, E.,

Neff, J. C., Schuur, E. A., and Zender, C. S.: The impact of boreal forest fire on climate warming, Science, 314, 1130–1132, 2006.
Rienecker, M. M., Suarez, M. J., Gelaro, R., Todling, R., Bacmeister, J., Liu, E., Bosilovich, M. G., Schubert, S. D., Takacs, L., Kim, G.-K., Bloom, S., Chen, J., Collins, D., Conaty, A., da Silva, A., Gu, W., Joiner, J., Koster, R. D., Lucchesi, R., Molod, A., Owens, T., Pawson, S., Pegion, P., Redder, C. R., Reichle, R., Robertson, F. R., Ruddick, A. G., Sienkiewicz, M., and Woollen, J.: MERRA: NASA's Modern-Era Retrospective Analysis for Research and Applications, J. Climate, 24, 3624–3648, doi:10.1175/JCLI-D-11-00015.1, 2011.
Roy, D. P., Boschetti, L., Justice, C. O., and Ju, J.: The collection 5 MODIS burned area product – global evaluation by comparison with the MODIS active fire product, Remote Sens. Environ., 112, 3690–3707, 2008.
Running, S. W.: Ecosystem disturbance, carbon, and climate, Science, 321, 652–653, 2008.
Rupp, T. S., Xi Chen, Olson, M., and McGuire, A. D.: Sensitivity of simulated boreal fire dynamics to uncertainties in climate drivers, Earth Interact., 11, 1–21, 2007.
Ryan, K. C.: Dynamic interactions between forest structure and fire behavior in boreal ecosystems, Silva Fenn., 36, 13–39, 2002.
Saatchi, S. S., Harris, N. L., Brown, S., Lefsky, M., Mitchard, E. T. A., Salas, W., Zutta, B. R., Buermann, W., Lewis, S. L., Hagen, S., Petrova, S., White, L., Silman, M., and Morel, A.: Benchmark map of forest carbon stocks in tropical regions across three continents, P. Natl. Acad. Sci. USA, 108, 9899–9904, doi:10.1073/pnas.1019576108, 2011.
Sastry, N.: Forest fires, air pollution, and mortality in Southeast Asia, Demography, 39, 1–23, doi:10.1353/dem.2002.0009, 2002.
Schumaker, N. H.: Using landscape indices to predict habitat connectivity, Ecology, 77, 1210–1225, 1996.
Scott, J. H. and Burgan, R. E.: Standard fire behavior fuel models: a comprehensive set for use with Rothermel's surface fire spread model, Gen. Tech. Rep. RMRS-GTR-153m Fort Collins, CO: U.S. Department of Agriculture, Forest Service, Rocky Mountain Research Station, 72 p., 2005.
Sedano, F. and Randerson, J. T.: Vapor pressure deficit controls on fire ignition and fire spread in boreal forest ecosystems, Biogeosciences Discuss., 11, 1309–1353, doi:10.5194/bgd-11-1309-2014, 2014.

Serreze, M. C. and Hurst, C. M.: Representation of mean arctic precipitation from NCEP–NCAR and ERA reanalyses, J. Climate, 13, 182–201, 2000.
Sitch, S., Smith, B., Prentice, I. C., Arneth, A., Bondeau, A., Cramer, W., Kaplan, J. O., Levis, S., Lucht, W., Sykes, M. T., Thonicke, K., and Venevsky, S.: Evaluation of ecosystem dynamics, plant geography and terrestrial carbon cycling in the LPJ dynamic global vegetation model, Glob. Change Biol., 9, 161–185, doi:10.1046/j.1365-2486.2003.00569.x, 2003.
Soares-Filho, B., Silvestrini, R., Nepstad, D., Brando, P., Rodrigues, H., Alencar, A., Coe, M., Locks, C., Lima, L., Hissa, L., and Stickler, C. H.: Forest fragmentation, climate change and understory fire regimes on the Amazonian landscapes of the Xingu headwaters, Landscape Ecol., 27, 585–598, 2012.
Spessa, A., van der Werf, G., Thonicke, K., Gomez Dans, J., Lehsten, V., Fisher, R., and Forrest, M.: Modeling Vegetation Fires and Fire Emissions, available at: http://oro.open.ac.uk/39953/ (last access: 22 May 2014), 2013.
Stocker, T. F., Dahe, Q., and Plattner, G.-K.: Climate Change 2013: The Physical Science Basis, Working Group I Contribution to the Fifth Assessment Report of the Intergovernmental Panel on Climate Change. Summary for Policymakers, available at: http://www.climatechange2013.org/images/report/WG1AR5_Frontmatter_FINAL.pdf (last access: 28 February 2014), IPCC, 2013.
Stocks, B. J., Mason, J. A., Todd, J. B., Bosch, E. M., Wotton, B. M., Amiro, B. D., Flannigan, M. D., Hirsch, K. G., Logan, K. A., Martell, D. L., and Skinner, W. R.: Large forest fires in Canada, 1959–1997, J. Geophys. Res., 107, 8149, doi:10.1029/2001JD000484, 2002.
Taylor, K. E., Stouffer, R. J., and Meehl, G. A.: An overview of CMIP5 and the experiment design, B. Am. Meteorol. Soc., 93, 485–498, 2012.
Thomson, A. M., Calvin, K. V., Chini, L. P., Hurtt, G., Edmonds, J. A., Bond-Lamberty, B., Frolking, S., Wise, M. A., and Janetos, A. C.: Climate mitigation and the future of tropical landscapes, P. Natl. Acad. Sci. USA, 107, 19633–19638, doi:10.1073/pnas.0910467107, 2010.
Thonicke, K., Venevsky, S., Sitch, S., and Cramer, W.: The role of fire disturbance for global vegetation dynamics: coupling fire into a dynamic Global Vegetation Model, Global Ecol. Biogeogr., 10, 661–677, 2001.
Thonicke, K., Spessa, A., Prentice, I. C., Harrison, S. P., Dong, L., and Carmona-Moreno, C.: The influence of vegetation, fire spread and fire behaviour on biomass burning and trace gas emissions: results from a process-based model, Biogeosciences, 7, 1991–2011, doi:10.5194/bg-7-1991-2010, 2010.

BGD
11, 10779–10826, 2014
HESFIRE
Y. Le Page et al.

Thrupp, L. A., Hecht, S., Browder, J. O., and Institute, W. R.: The Diversity and Dynamics of Shifting Cultivation: Myths, Realities, and Policy Implications, World Resources Institute, 1997.

Tilman, D., Balzer, C., Hill, J., and Befort, B. L.: Global food demand and the sustainable intensification of agriculture, P. Natl. Acad. Sci. USA, 108, 20260–20264, doi:10.1073/pnas.1116437108, 2011.

Van Vuuren, D. P., Edmonds, J., Kainuma, M., Riahi, K., Thomson, A., Hibbard, K., Hurtt, G. C., Kram, T., Krey, V., and Lamarque, J.-F.: The representative concentration pathways: an overview, Climatic Change, 109, 5–31, 2011.

van der Werf, G. R., Dempewolf, J., Trigg, S. N., Randerson, J. T., Kasibhatla, P. S., Giglio, L., Murdiyarso, D., Peters, W., Morton, D. C., and Collatz, G. J.: Climate regulation of fire emissions and deforestation in equatorial Asia, P. Natl. Acad. Sci. USA, 105, 20350–20355, 2008.

van der Werf, G. R., Randerson, J. T., Giglio, L., Collatz, G. J., Mu, M., Kasibhatla, P. S., Morton, D. C., DeFries, R. S., Jin, Y., and van Leeuwen, T. T.: Global fire emissions and the contribution of deforestation, savanna, forest, agricultural, and peat fires (1997–2009), Atmos. Chem. Phys., 10, 11707–11735, doi:10.5194/acp-10-11707-2010, 2010.

Westerling, A. L., Cayan, D. R., Brown, T. J., Hall, B. L., and Riddle, L. G.: Climate, Santa Ana winds and autumn wildfires in southern California, EOS T. Am. Geophys. Un., 85, 289–296, 2004.

BGD
11, 10779–10826, 2014
HESFIRE
Y. Le Page et al.

Table 1. Model parameters.

Parameter	Description	Value and unit	Optimization range
Ignitions			
CG_{firep}	Average probability of ignition from a cloud-to-ground lightning strike on natural vegetation.	6.8 %	[2.8–16.6]
LUign	Original number of human ignitions per km^2 of land use per 24 h, prior to applying density-decreasing function (see LUexp).	2.3×10^{-3} km^{-1}	$[1.1–6] \times 10^{-3}$
LUexp	Shape parameter: controls the decreasing contribution of incremental land use areas to human ignitions.	14.9	[14.7–19.8]
GDP_{exp} [a]	Shape parameter: impact of GDP on ignitions, through land use practices.	1.28	[0.83–3.02]
LU_{range}	Range of fractional land use controlling human ignitions, with no ignitions beyond the upper bound.	[0–0.1]	–
GDP_{range}	Range of regional GDP controlling fire ignitions, through land use practices.	[0–60 000] \$ cap^{-1} yr^{-1}	–
Spread			
BAfrag	Delay before burned areas can burn again, meanwhile contributing to fragmentation.	8 months	–
$Max_{forestrate}$	Maximum fire spread rate in forests.	0.28 m s^{-1}	–
$Max_{shrubrate}$	Maximum fire spread rate in shrublands.	1.12 m s^{-1}	–
$Max_{grassrate}$	Maximum fire spread rate in grasslands.	2.79 m s^{-1}	–
RH_{range}	Range of relative humidity controlling fire spread.	[30 80]%	–
RH_{exp}	Shape parameter: impact of relative humidity on fire spread rate.	1.18	[0.52–1.31]
SW_{range}	Range of volumetric soil moisture controlling fire spread.	[20 35]%	–
SW_{exp}	Shape parameter: impact of volumetric soil moisture on fire spread rate.	1.21	[0.30–1.44]
T_{range}	Range of temperature controlling fire spread.	[0 30] °C	–
T_{exp}	Shape parameter: impact of air temperature on fire spread rate.	1.78	[0.8–3.8]
Termination			
$Fuel_{range}$	Range of precipitation controlling termination probability, through fuel build-up.	[0.5 3] mm day^{-1}	–
Fuelspan	Timespan of average precipitation controlling fuel build-up.	12 months	–
Fueldelay	Delay from actual precipitation to fuel build-up.	3 months	–
$Fuel_{exp}$	Shape parameter: impact of precipitation over −15 to −3 months on fire termination probability, a proxy fuel build-up.	1.72	[1.62–3.65]
$Frag_{range}$	Range of fractional landscape fragmentation controlling termination probability.	[0 1]	–
$Frag_{exp}$	Shape parameter: impact of landscape fragmentation on fire termination probability.	1.81	[0.94–2.48]
LU_{range}	Range of fractional land use controlling termination probability, through suppression efforts.	[0 0.1]	–
$LUSUP_{exp}$	Shape parameter: impact of land use on fire termination probability, through suppression efforts, in interaction with GDP (below).	4.08	[1.62–7.18]
GDP_{range}	Range of regional GDP controlling fire suppression effort.	[0–60 000] \$ cap^{-1} yr^{-1}	–
GDP_{exp} [a]	Shape parameter: impact of GDP on suppression effort, through land use practices.	1.28	[0.83–3.02]

[a] In order to limit the number of parameters to optimize for the first version of the fire model, GDP_{exp} is attributed the same optimized value whether it applies to fire ignitions or fire termination.

BGD
11, 10779–10826, 2014
HESFIRE
Y. Le Page et al.

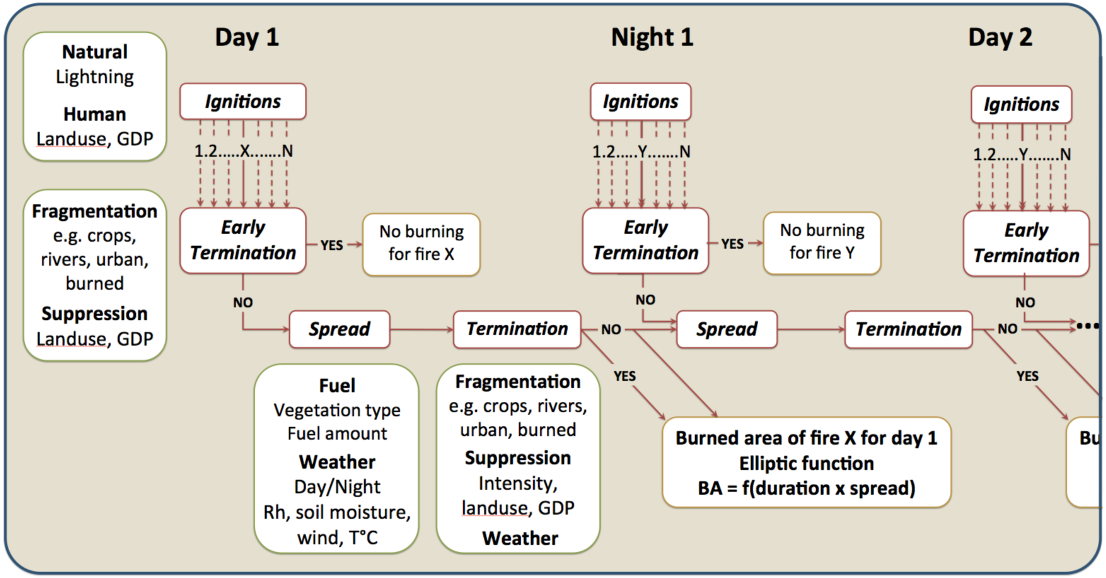

Figure 1. HESFIRE diagram.

BGD
11, 10779–10826, 2014

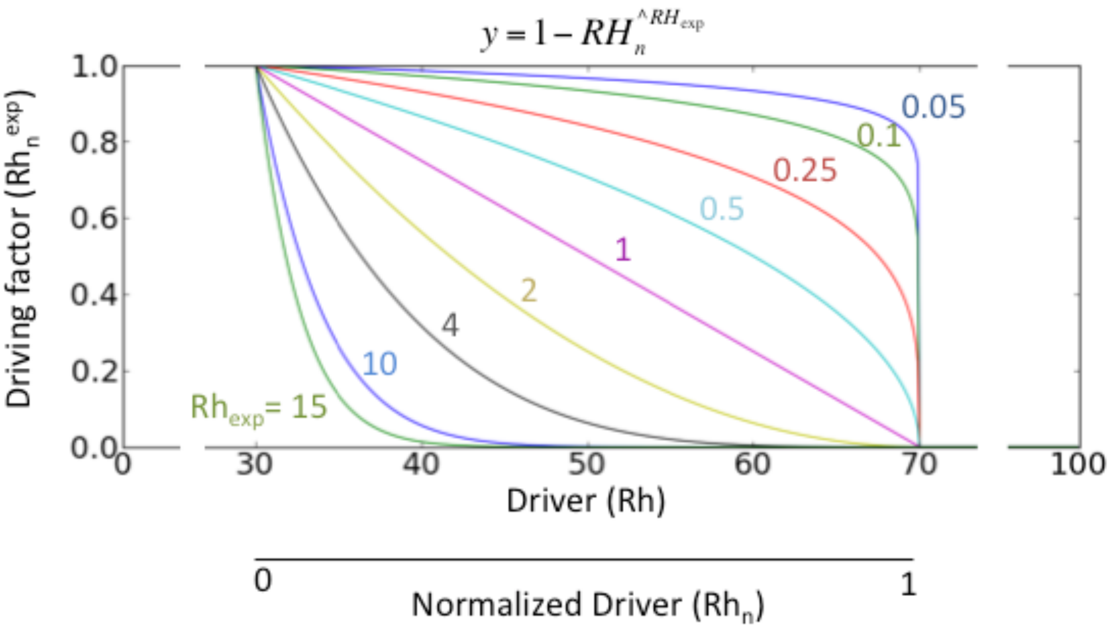

Figure 2. Control of shape parameters (exponents, here RH_{exp}) on fire driving relationships. The exponent can take any value (from 0.033 to 30) as determined by the optimization procedure, thus covering a wide space of potential fire-driving influence.

BGD
11, 10779–10826, 2014

HESFIRE

Y. Le Page et al.

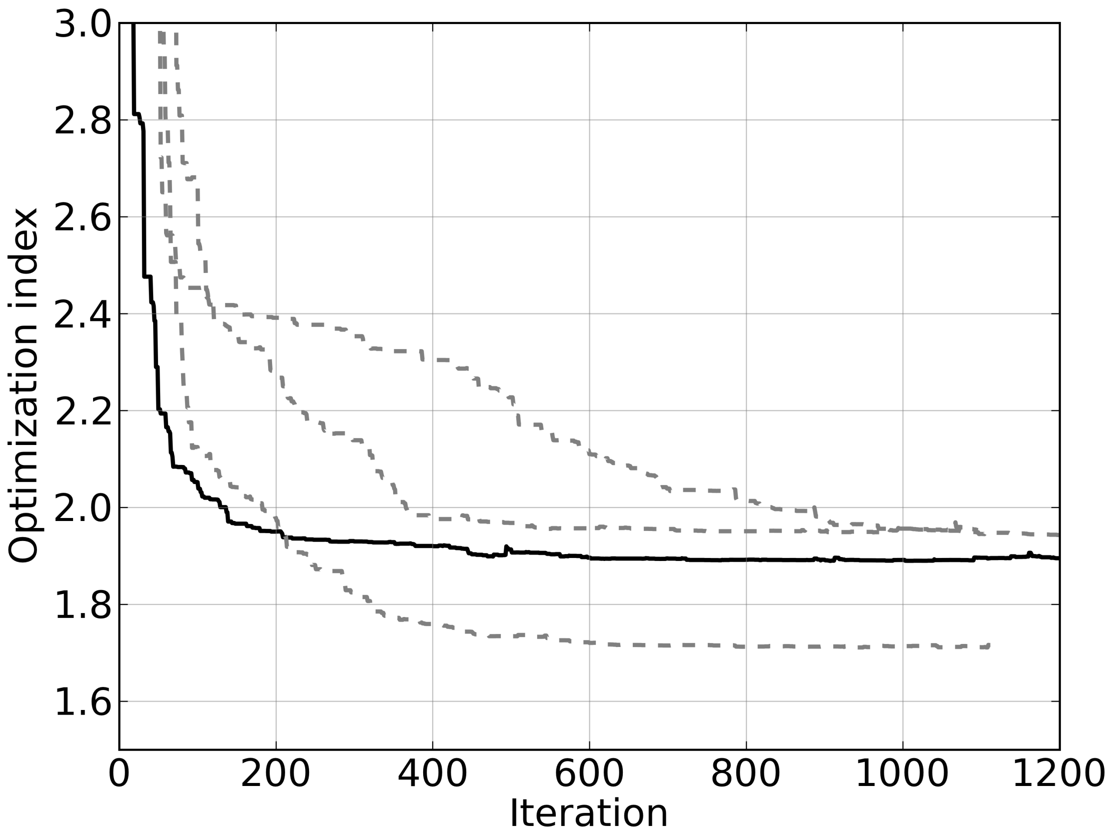

Figure 3. HESFIRE's performance through the optimization procedure iterations. The solid line represents the optimization of the final model (which happened to reach a near-final parameterization quite rapidly). The dashed lines represent the optimization of three of the alternative runs, using different sets of grid-cells and years to evaluate the robustness of the parameters.

BGD
11, 10779–10826, 2014

HESFIRE

Y. Le Page et al.

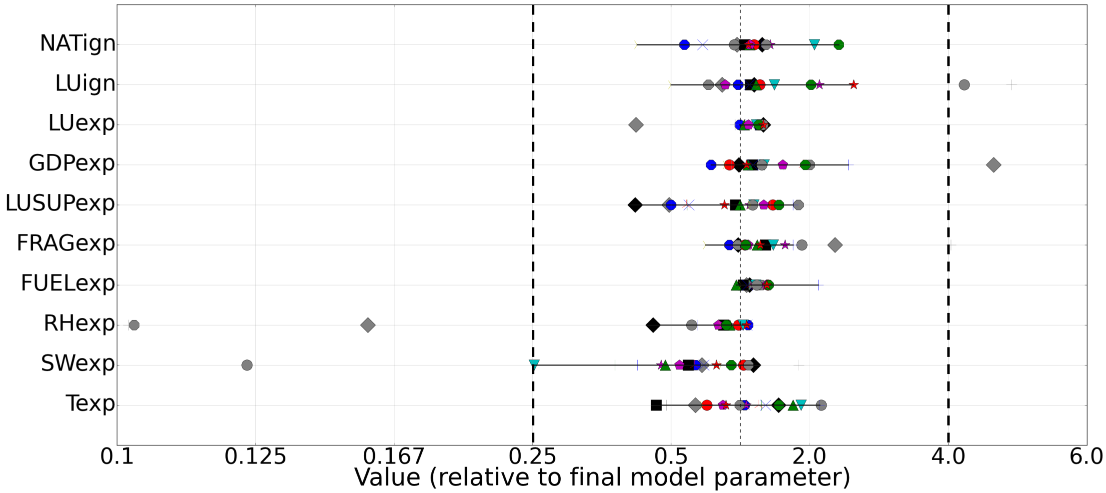

Figure 4. Parameter variability across the 20 optimization runs, each with a different time span and grid-cell subset. Among the 20 runs, 16 reached a relatively consistent parameterization (see text). These are represented as colored markers and their range is shown by the black horizontal lines. For the other 4 runs, parameters are shown as grey markers. The vertical dashed lines indicate the lower and upper thresholds which were used to tease apart these 4 runs.

Discussion Paper | Discussion Paper | Discussion Paper | Discussion Paper |

BGD

11, 10779–10826, 2014

HESFIRE

Y. Le Page et al.

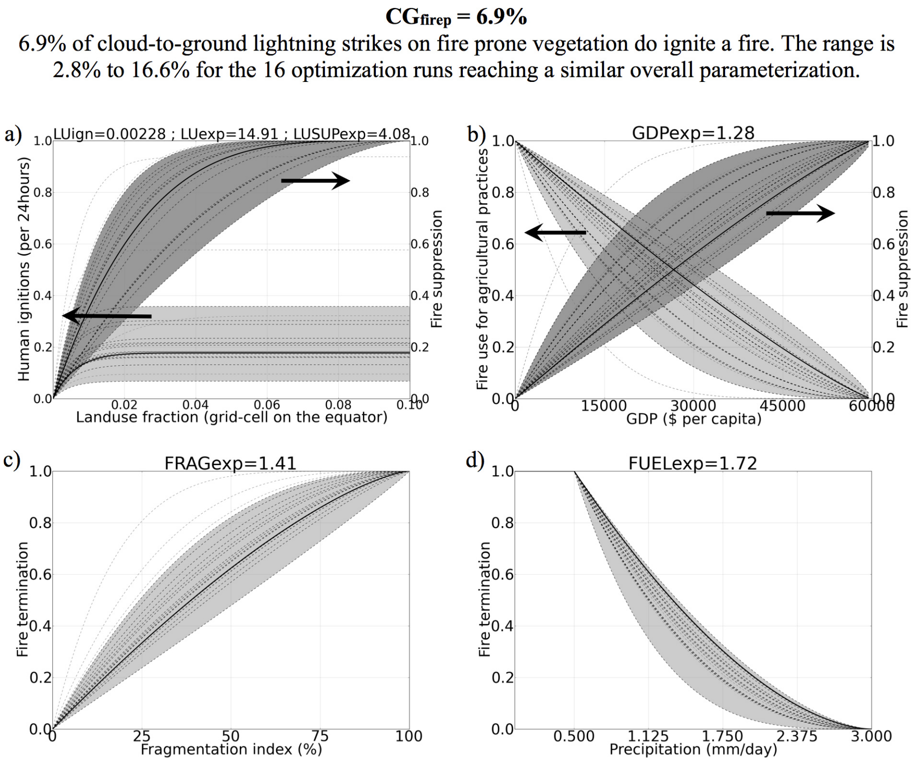

Figure 5. Optimized model parameters and their influence on fire ecology. For each plot, the thick black line represents the parameter influence in the final model. The dotted black lines represent the 16 optimization runs that reached a similar parameterization to the final model, the shaded area showing the range of their influence. The dotted grey lines represent the four optimization runs which reached a parameterization substantially different from the final model (see text).

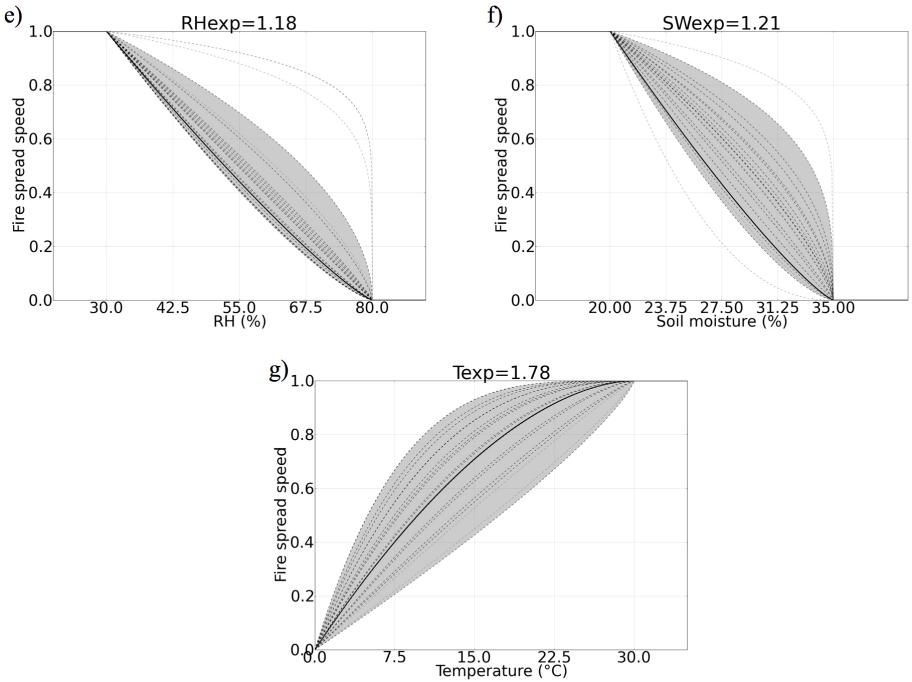

Figure 5. Continued.

BGD
11, 10779–10826, 2014

HESFIRE

Y. Le Page et al.

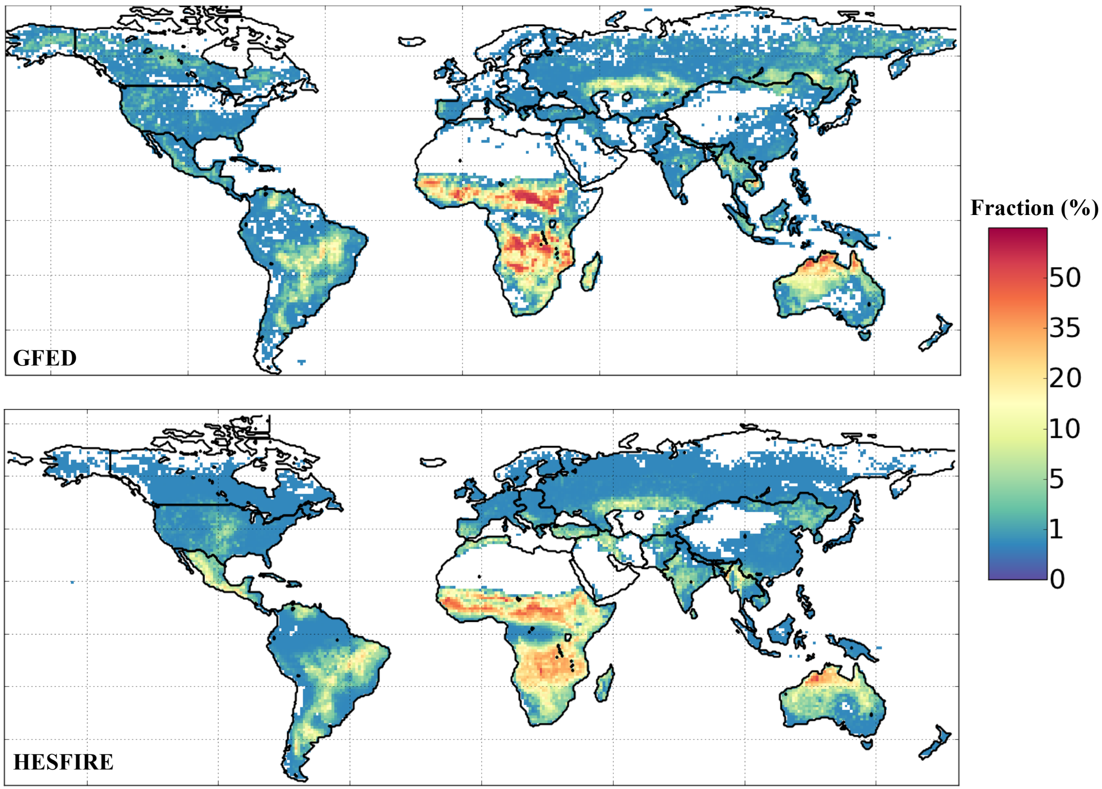

Figure 6. Observed and modeled average annual burned fraction. Top: GFEDv3 burned areas on "natural" landscapes. Bottom: fire model.

BGD
11, 10779–10826, 2014
HESFIRE
Y. Le Page et al.

Title Page
Abstract Introduction
Conclusions References
Tables Figures
Back Close
Full Screen / Esc
Printer-friendly Version
Interactive Discussion

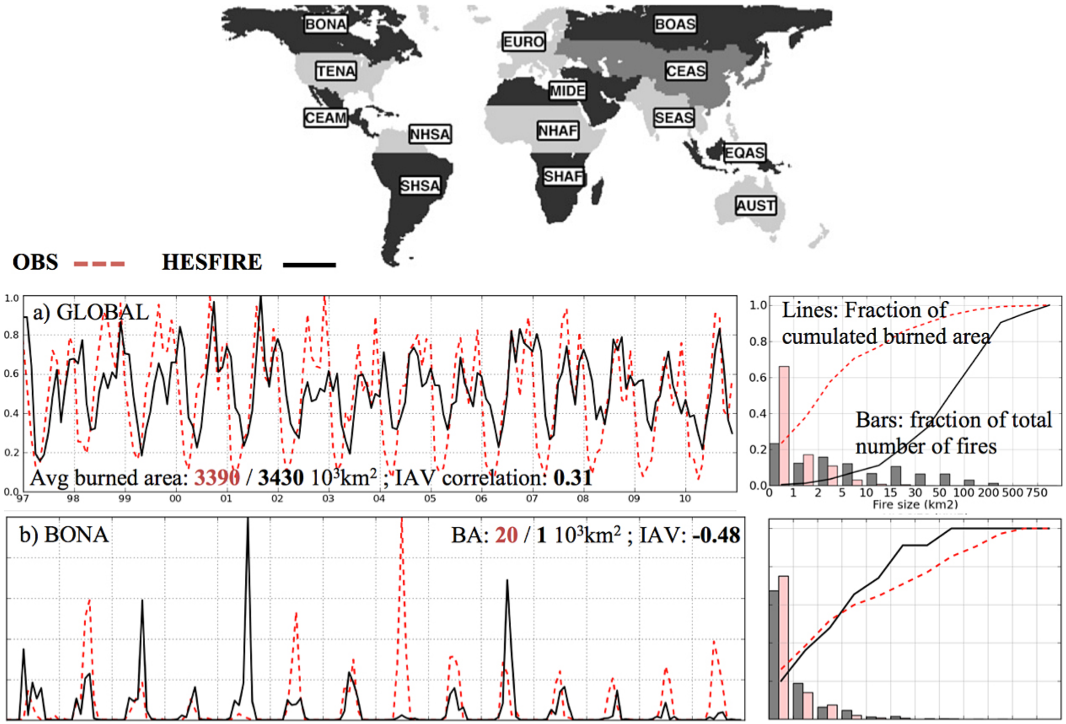

Figure 7. Comparison of HESFIRE with observation-derived data over 14 regions. Left side plots: time series of normalized monthly burned area, with quantification of average annual burned area in GFED and in HESFIRE, and inter-annual correlation. Right side: 2005 distribution of fires by size classes and cumulative burned area along these classes. Observation data are from the MODIS MCD45 product.

BGD
11, 10779–10826, 2014

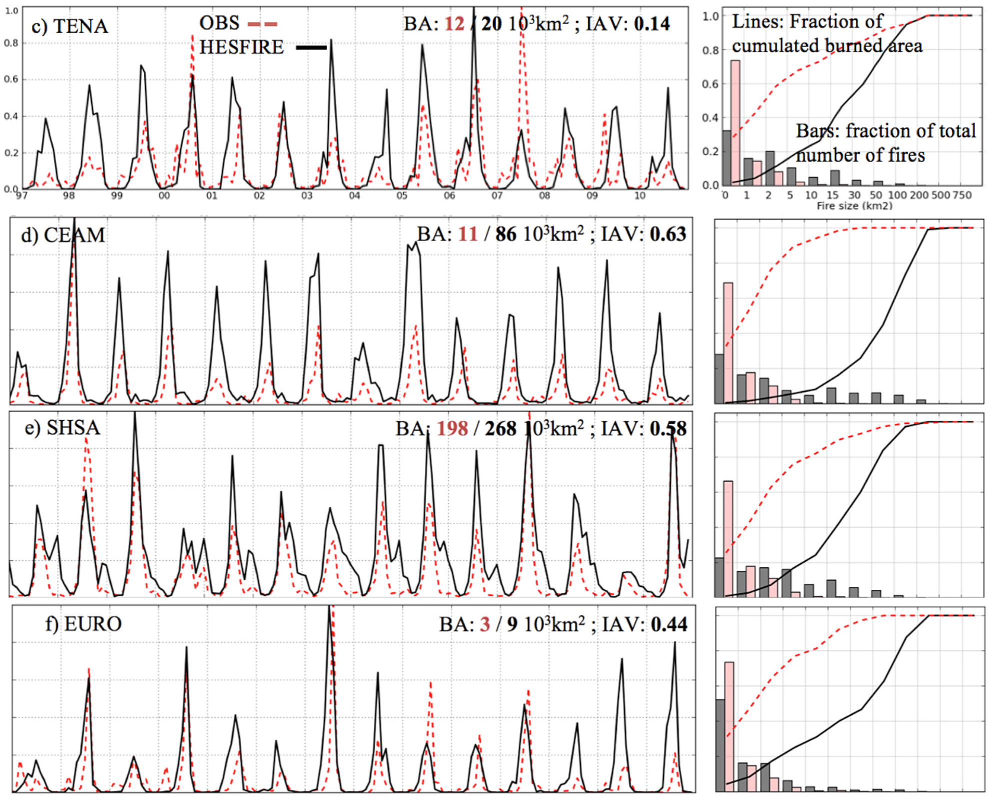

Figure 7. Continued.

BGD
11, 10779–10826, 2014
HESFIRE
Y. Le Page et al.

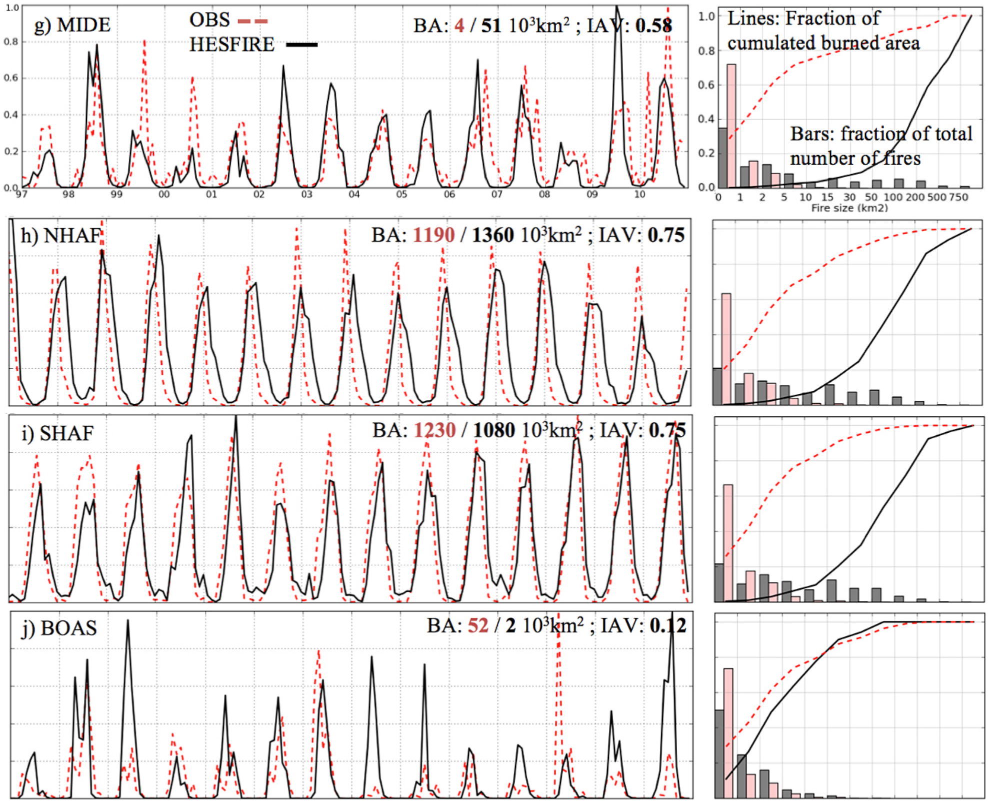

Figure 7. Continued.

BGD
11, 10779–10826, 2014
HESFIRE
Y. Le Page et al.

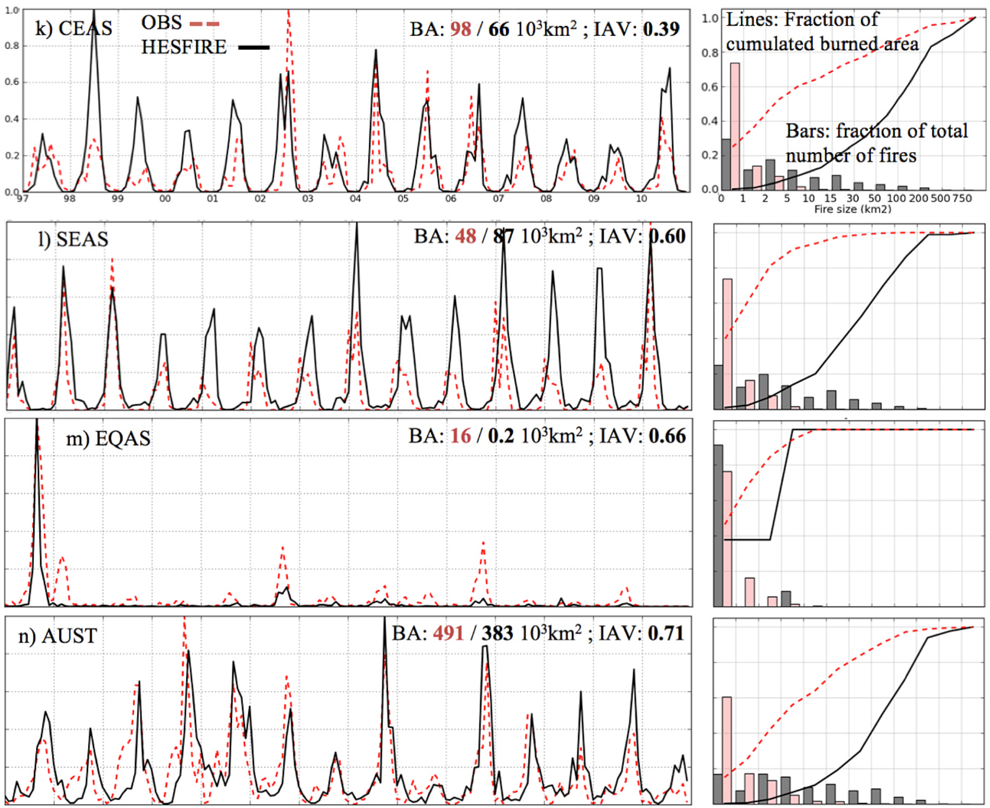

Figure 7. Continued.

BGD
11, 10779–10826, 2014

HESFIRE

Y. Le Page et al.

Title Page
Abstract
Introduction
Conclusions
References
Tables
Figures
◀
▶
Back
Close
Full Screen / Esc
Printer-friendly Version
Interactive Discussion

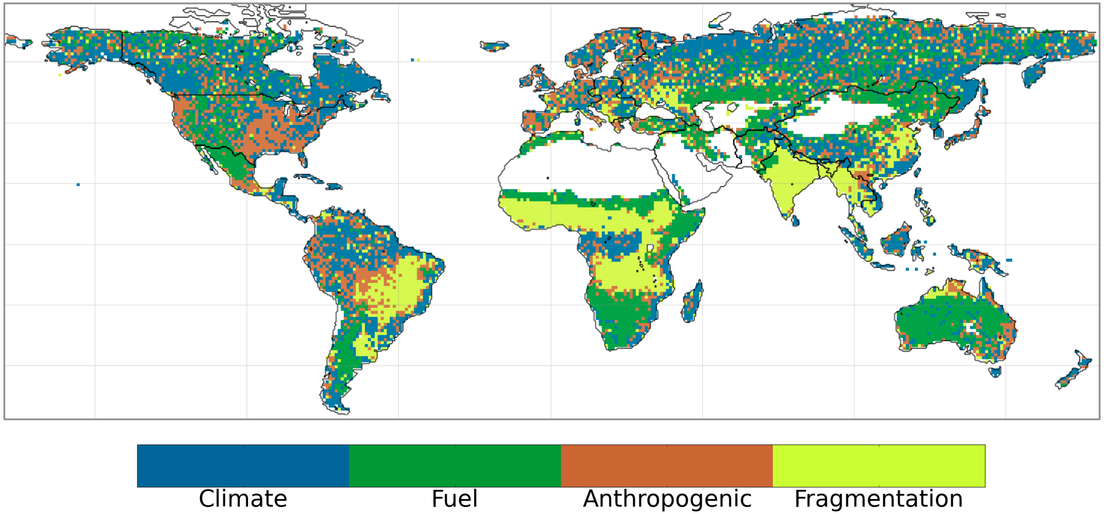

Figure 8. Major drivers of average annual burned area sensitivity among the 9 optimized parameters as grouped into 4 thematic classes (climate, vegetation fuel, anthropogenic practices, landscape fragmentation). For each of the 9 parameters, HESFIRE was run keeping the original parameterization, but altering the value of the considered parameter by -50 % and +50 %. The map shows the class of the parameter for which the average burned area in the considered grid-cell varied the most between the 2 runs with these alternative values.

BGD
11, 10779–10826, 2014
HESFIRE
Y. Le Page et al.